Precambrian Research 403 (2024) 107327

Contents lists available at ScienceDirect

Precambrian Research

journal homepage: www.elsevier.com/locate/precamres

Xenocrystic zircons from mafic volcanic rocks in the Bikou Terrane: A window to trace the Paleoarchean to Mesoproterozoic crustal evolution of the northwestern Yangtze Block, South China

Bo Hui [a], Yunpeng Dong [a,b,*], Hongjun Qu [a], Shengsi Sun [a], Franz Neubauer [c], Feifei Zhang [a], Rutao Zang [a], Shuxuan Yan [a], Guiyun Wang [a]

[a] State Key Laboratory of Continental Dynamics, Department of Geology, Northwest University, Northern Taibai Str.229, Xi'an 710069, China
[b] Collaborative Innovation Research Centre of Continental Tectonics, Northwest University, Northern Taibai Str.229, Xi'an 710069, China
[c] Department of Environment and Biodiversity, Geology Division, Paris Lodron-University of Salzburg, Hellbrunnerstr. 34, 5020 Salzburg, Austria

ARTICLE INFO

Keywords:
Yangtze Block
Bikou Terrane
Paleoarchean to Mesoproterozoic
Xenocrystic zircon
Crustal evolution

ABSTRACT

The early crustal properties of the northwestern Yangtze domain are a crucial puzzle piece in elucidating the Archean to Mesoproterozoic crustal evolution of the Yangtze Block. However, related comprehension remains constrained by the scarcity of surface exposures. The accidental discovery of xenocrystic zircons in the Bikou Terrane offers valuable insights into the information of the deep crust in the region. This study presents systematic zircon U–Pb geochronology, zircon Hf isotopes and whole-rock geochemistry on this specific set of mafic *meta*-volcanic rocks identified from the Bikou Terrane. The zircon properties, alongside the dating results, indicate a xenocrystic origin for all the extracted zircons, with ages scattered at ca. 3.50, 2.88 and 2.72–2.62 Ga in the Archean, ca. 2.52–2.37, 2.23–2.16, 2.07–1.95 and 1.90–1.77 Ga in the Paleoproterozoic, ca. 1.16–1.05 Ga in the Mesoproterozoic and ca. 820 Ma in the Neoproterozoic. The youngest zircon age clusters, plus the regional geological fact that the Bikou Group was covered by the Cryogenian, indicate their formation in the late Tonian. The geochemical fingerprints demonstrate the OIB-like nature of the mafic magma but with apparent Nb-Ta depletion, confirming their deep-seated crustal contamination. Combining Hf isotopic analysis reveals that the xenocrystic zircons not only encompass the information reflected in the Yudongzi Complex but also preserve additional new imprints pointing to the presence of a unified deep crust within the Bikou Terrane and a more intricate early evolutionary history. An intergraded examination of the early geological records in the northwestern Yangtze Block reveals multiple early crustal evolution events, including pulsed crustal growth/reworking at ca. 3.50, 2.88–2.78 and 2.72–2.62 Ga in the Paleoarchean–Neoarchean, ancient crust reworking at ca. 2.52–2.37 and 2.23–2.16 Ga plus reworking alongside high-grade metamorphism at ca. 2.07–1.95 Ga in the early Paleoproterozoic, followed by recycling events involving new component at ca. 1.90–1.76 and 1.16–1.05 Ga in the latest Paleo- and Mesoproterozoic, respectively. Comparative considerations indicate a discrete history in various Yangtze domains during the Archean, gradually converging by the early Paleoproterozoic. The latest Paleo- and Mesoproterozoic brought allied crustal remelting and vertical accretion, implying the potential unity of the Yangtze Block by the late Paleoproterozoic.

1. Introduction

Episodic tectono-thermal events during the Archean to Mesoproterozoic play a pivotal role in tracing Earth's early crustal evolution (Condie et al., 2011; Zheng et al., 2013; Hawkesworth et al., 2017; Moyen et al., 2017). These globally crucial occurrences contributed significantly to the formation of continental crust throughout the Archean–Mesoproterozoic period in diverse landmasses across the globe (e.g., Hoffman, 1989; Zhao et al., 2002; Zhai et al., 2005; O'Reilly et al., 2008; Gao et al., 2011). Compared to areas characterized by abundant geological records and extensive surface exposures, exploring blocks featuring restricted Archean–Mesoproterozoic rock exposures poses a

* Corresponding author at: State Key Laboratory of Continental Dynamics, Department of Geology, Northwest University, Northern Taibai Str.229, Xi'an 710069, China.
E-mail address: dongyp@nwu.edu.cn (Y. Dong).

https://doi.org/10.1016/j.precamres.2024.107327
Received 16 November 2023; Received in revised form 8 January 2024; Accepted 7 February 2024
Available online 17 February 2024

challenging task. This is because the limited surface geological records may not fully convey comprehensive information about the deep concealed crust (Miller et al., 2007; Stern et al., 2010; Condie et al., 2011; Hawkesworth et al., 2017). As a prevalent mineral in continental crustal rocks, zircon is renowned for its relative stability against diverse physiochemical processes, even when exposed to the relatively harsh conditions of the Earth's mantle. This makes zircon a vital mineral that has endured since the Earth's earliest geological epochs (Belousova et al., 2002; Wu and Zheng, 2004; Siebel et al., 2009; Kemp et al., 2010). In this context, xenocrystic zircons, especially those hosted in mantle-derived deep-seated mafic magma, constitute an excellent carrier that records relevant information about the Earth's deep crust. This unique perspective offers a valuable tool for deciphering Archean–Mesoproterozoic tectono-thermal events that might not be evident in surface geological records (e.g., Griffin et al., 2000; Siebel et al., 2009; Kemp et al., 2010; Stern et al., 2010; Zheng et al., 2012; Zhang et al., 2015; Chaudhuri et al., 2018). Therefore, extracting relevant information from xenocrystic zircons is able to provide a deeper comprehension of the early crustal evolution within the continental crust.

The Yangtze Block stands as a pivotal Precambrian craton in the southern part of mainland China (Fig. 1). The limited surface exposures of Archean to Mesoproterozoic rocks are primarily confined to the northern, northwestern and southwestern domains. Contemporary research endeavors have mostly centered on the north and southwest of the Yangtze Block, which preserve a wealth of diverse rock types, spanning a broad temporal range and featuring extensive distribution of Archean to Mesoproterozoic rocks (e.g., Gao et al., 1999; Zhang et al., 2006a; Zheng et al., 2006; Zhang and Zheng, 2013; Guo et al., 2014a; Zhu et al., 2016; Hui et al., 2017; Zhou et al., 2017; Wang and Dong, 2019; Cui et al., 2020; Liu et al., 2020). This geological diversity serves as a robust scientific foundation for investigating the nature of early continental crust and its evolution in the northern and southwestern domains. Corresponding interpretations outlining the early crustal evolution have been established within the academic community for these areas (e.g., Gao et al., 2011; Zhao and Cawood, 2012; Cawood et al., 2020; Wang et al., 2020; Zhao et al., 2020; Liu et al., 2021). Conversely, the record on the northwestern domain is notably limited, with only sporadic exposures such as the Yudongzi Complex in the Bikou Terrane and the Houhe Complex in the Hannan-Micangshan Massif (Fig. 1). Despite proactive research efforts on these geological units, whether these outcrops can fully document the nature of the deep crust on the northwestern domain still awaits new evidence to provide substantial support (Wu et al., 2012; Hui et al., 2017, 2019; Zhou et al., 2018; Chen et al., 2019; Zhang et al., 2020). Moreover, the inquiry into whether the northwestern Yangtze Block underwent a similar Archean to Mesoproterozoic crustal evolution, akin to the processes observed in the northern and southwestern domains, remains a critical question (Zhao and Cawood, 2012; Hui et al., 2017, 2019; Zhou et al., 2018; Wang et al., 2020; Cawood et al., 2020; Zhang et al., 2020). These motivations drive us to necessitate in-depth and comprehensive comparative analyses, as the resolution of this query profoundly impacts our understanding of the tectonic properties of the Yangtze Block. Fortuitously, a substantial number of xenocrystic zircons have been discovered in our recent studies of the mafic *meta*-volcanic rocks within the Bikou Group of the Bikou Terrane. Such a finding offers an invaluable window to trace the early crustal properties governing its evolution

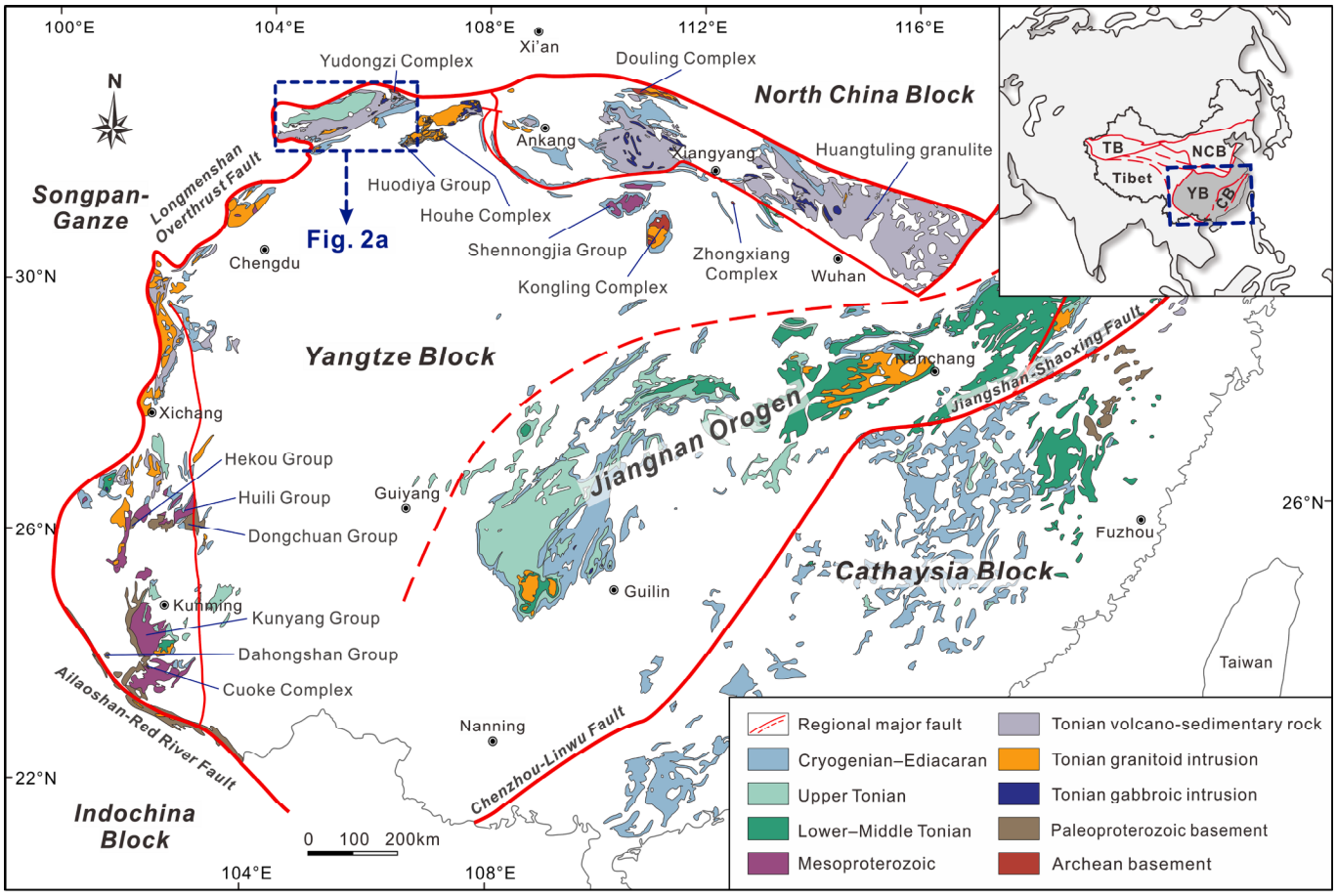

Fig. 1. A sketch geological map highlighting the distribution of major Precambrian rocks in the Yangtze Block (after Dong et al., 2024a). Insert map at the top-right corner showing major tectonic blocks in the southeastern Eurasia continent and the location of the Yangtze Block. Abbreviations: CB, Cathaysia Block; NCB, North China Block; TB, Tarim Block; YB, Yangtze Block.

on the Yangtze northwestern domain.

This study presents zircon U–Pb dating, zircon Hf isotopic and whole-rock geochemical data from the mafic *meta*-volcanic rocks within the Bikou Group. The new contributions, combined with surface rock databases, not only empower to conduct an in-depth investigation into the Archean to Mesoproterozoic crustal evolution on the northwestern domain of the Yangtze Block, but also allow for a comprehensive comparison with the early crustal properties of the northern and southwestern domains of the Yangtze Block.

2. Geological background

The Yangtze Block occupies the southeastern extent of the Eurasia continent and constitutes one of the most ancient Precambrian blocks in mainland China (Fig. 1). It is juxtaposed against the Songpan-Ganze Terrane by the Longmenshan Overthrust Fault to the west, and against the Indochina Block by the Ailaoshan-Red River Fault to the southwest. To the north, it is separated from the North China Block by the Qinling-Dabie-Sulu Orogen, whereas to the east, it is in contact with the Cathaysia Block by the Jiangshan-Shaoxing Fault (Fig. 1). The Yangtze Block has experienced a long and complex evolutionary history since the Archean. It contains abundant Precambrian records, including the Archean–Paleoproterozoic basement, Mesoproterozoic *meta*-sedimentary strata, early Neoproterozoic plutonic complex and volcano-sedimentary sequences, and middle–late Neoproterozoic cover (Fig. 1).

The Archean–Paleoproterozoic basement contains the Kongling (ca. 3.45–1.78 Ga; e.g., Zhang et al., 2006a; Gao et al., 2011; Guo et al., 2014a, 2015), Zhongxiang (ca. 2.90–1.82 Ga; e.g., Wang et al., 2016; Zhou et al., 2017; Wang and Dong, 2019), Douling (ca. 2.51–2.41 Ga; e.g., Hu et al., 2013; Wu et al., 2014; Nie et al., 2016) and Huangtuling (ca. 2.72–1.98 Ga; e.g., Sun et al., 2008; Wu et al., 2008) complexes in the north, the Yudongzi (ca. 2.82–1.85 Ga; e.g., Hui et al., 2017, 2019) and Houhe (ca. 2.09–1.76 Ga; e.g., Wu et al., 2012; Deng et al., 2020) complexes in the northwest, and the Cuoke Complex (ca. 3.11–1.72 Ga, e.g., Cui et al., 2020; Liu et al., 2021; Yang et al., 2023) in the southwest. They consist mainly of amphibolite-facies tonalitic-trondhjemitic-granodioritic (TTG) gneisses, granitoid gneisses and amphibolites plus supracrustal rocks, recording continuous pulses of Archean crustal growth/reworking, and Paleoproterozoic tectono-thermal events in response to the assembly and breakup of the supercontinent Nuna (Columbia) (e.g., Gao et al., 2011; Zhao and Cawood, 2012; Zheng et al., 2013; Hui et al., 2017). The Paleoproterozoic supracrustal rocks crop out as the Dahongshan, Dongchuan, Tong'an and Hekou groups on the southwestern margin (Zhao et al., 2010; Zhou et al., 2014). Rare volcanic interlayers constrain their depositional age at ca. 1.76–1.66 Ga (Greentree and Li, 2008; Chen et al., 2013a; Zhou et al., 2014; Lu et al., 2020). Some ca. 1.50 Ga basaltic layers occur in local sections within the Dongchuan Group, suggesting that the accumulation may continue until the earliest Mesoproterozoic (Fan et al., 2013; Lu et al., 2019).

The Mesoproterozoic *meta*-sedimentary strata are limitedly distributed on the northern, northwestern and southwestern margins (Fig. 1). They are termed the Shennongjia, Huodiya, Kunyang and Huili groups from north, northwest to southwest. Interlayered volcanic rocks within these groups limit their deposition age to ca. 1.18–1.01 Ga, during the latest Mesoproterozoic (Qiu et al., 2011; Li et al., 2013a; Wang et al., 2014; Zhu et al., 2016; Chen et al., 2018). The sedimentary facies differed, with the northern-northwestern and southwester margins dominated by carbonate platform facies and littoral-shallow marine facies, respectively (Geng et al., 2017).

The Yangtze Block collided with the Cathaysia Block to form a unified South China at ca. 820 Ma (Zhou et al., 2002; Zhao and Cawood, 2012; Wang et al., 2013a; Shu et al., 2019; Yao et al., 2019). The collision-welded and later lithosphere extension formed two distinct rock assemblages on the eastern fringe, including > 820 Ma subduction-collision-related and ca. 820–720 Ma rift-related rocks (Wang et al., 2013a; Shu et al., 2019; Yao et al., 2019; Hui et al., 2021a). Unlike the interior margin, the exterior margin is dominated by long-term subduction (western margin) or subduction-accretion (northern margin) in the early Neoproterozoic. The Andean-type subduction along the western margin formed numerous plutonic complexes and volcanic basins with ages of ca. 860–750 Ma (Li and Kinny, 2002; Zhou et al., 2002, 2006; Dong et al., 2022, 2024a). The subduction-accretion along the northern margin generated ca. 880–720 Ma plutonic intrusions in the Bikou, Hannan-Micangshan, Xiaomoling, Fenghuangshan, Douling and Huangling areas (Ling et al., 2006; Dong et al., 2011, 2012, 2017; Zhao and Zhou, 2008; Hui et al., 2020, 2021b, 2022a; Hui et al., 2022b), and ca. 780–730 Ma Bikou, Xixiang, Wudang and Suixian volcano-clastic complexes (Xu et al., 2002; Dong et al., 2021; He et al., 2022). The middle–late Neoproterozoic cover is mainly composed of Cryogenian glacial-interglacial and Ediacaran epi-continental marine successions, which unconformably overly the pre-Cryogenian rocks of the entire Yangtze Block (Dong et al., 2024a; Dong et al., 2024b).

3. Bikou Terrane and sampling

The Bikou Terrane constitutes a Yangtze-affinited micro-terrane located in the northwestern Yangtze Block (Hui et al., 2017, 2019). It occupies a triangular domain in the NE-SW direction, with three sides respectively bounded by the Mianlue Suture, Huya Fault and Qingchuan-Pingwu Fault (Fig. 2a). The Archean–Paleoproterozoic Yudongzi Complex, the Tonian Bikou Group, the latest Tonian Hengdan Group, the Tonian gabbroic–granitoid pluton and the Cryogenian–Ediacaran cover constitute the Precambrian records of the Bikou Terrane. The Yudongzi Complex crops out in the northern periphery and consists of TTG gneiss, granitic gneiss, amphibolite and supracrustal rocks (Hui et al., 2017). It mainly records ca. 2.82–2.78 Ga juvenile crust growth, ca. 2.70–2.63 Ga crustal growth and reworking, ca. 2.52–2.45 Ga reworking of ancient crust and ca. 1.85 Ga metamorphic events (Hui et al., 2017, 2019). The ca. 846–764 Ma Bikou Group comprises three lithologies of volcanic, pyroclastic and sedimentary rocks, which were commonly overprinted by upper greenschist-facies metamorphism (Zhao et al., 1990; Yan et al., 2003; Lai et al., 2007; Wang et al., 2008). The basic-intermediate volcanics have various geochemical characteristics, including island-arc basalt (IAB), oceanic island basalt (OIB) and enriched mid-ocean-ridge basalt (E-MORB) types; the acidic volcanics also show either extensional or subduction-related affinities (Xu et al., 2002; Yan et al., 2004a; Yan et al., 2004b; Lai et al., 2007; Wang et al., 2008). The diverse and complex compositions indicate the Bikou Group may form under a subduction-related system, associated with a back-arc extension (Hui et al., 2022a). Bounded by the Fengxiang-Tongqian Fault, the Hengdan Group, with a maximum depositional age at ca. 720 Ma, belongs to a gravity-flow deposits accumulated in a fore-arc basin (Hui et al., 2021c). The subduction-related gabbro and granitoid occur as tectonic lenses in the east part of the terrane with crystallization ages of ca. 880–824 Ma (Xiao et al., 2007; Wang et al., 2012; Li et al., 2013b; Ping et al., 2014; Hui et al., 2021b, 2022a). The Cryogenian–Ediacaran cover is sporadically exposed in the northern, southwestern and southeastern domains.

Field excursion and sampling in this study revolved around the Bikou Group along the Huangjiaping-Yinchang section (the A–B section marked in Fig. 2a) in the southern domain of the Bikou Terrane. Detailed field investigations reveal that the profile contains subordinate *meta*-volcanic rocks than dominating *meta*-pyroclastic and sedimentary rocks of the Bikou Group (Fig. 2b). Most of the rocks have been subjected to a degree of schistosity due to the greenschist-facies metamorphism. These rocks show a similar attitude dipping toward the southwest, consistent with the regional structure (Fig. 2b). Along the profile from the Huangjiaping to Yinchang, the lithology in the southwest is mainly composed of feldspathic quartzite, *meta*-tuffaceous sandstone and quartz schist, with some basic-intermediate *meta*-volcanics and tuffaceous interbeds appearing in the Dashanli area (Fig. 3a–c). In the section from Dashanli to Yinchangli, quartzite, feldspathic quartzite, silty phyllite

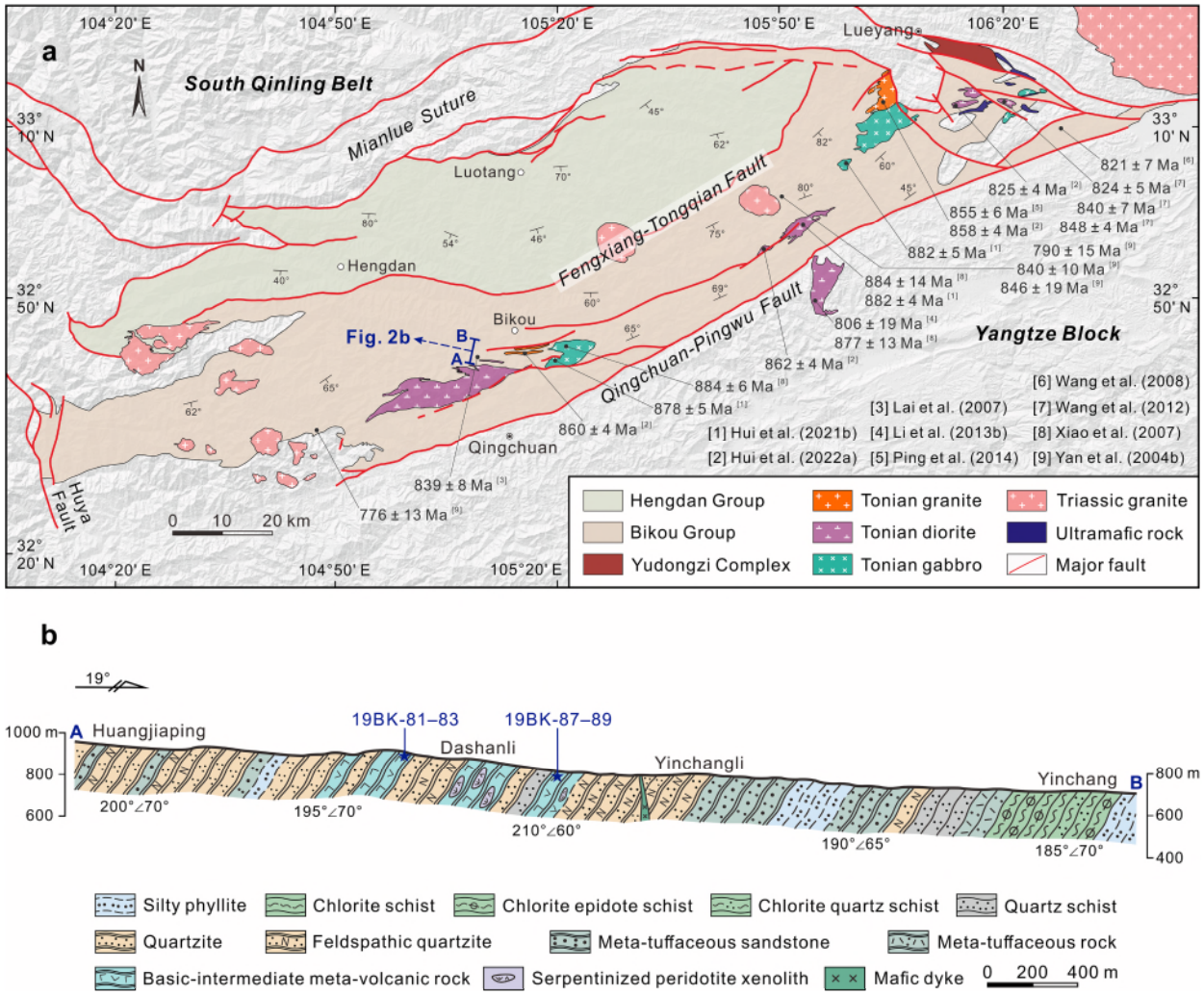

Fig. 2. (a) A simplified geological map of the Bikou Terrane (from Hui et al., 2022a); (b) A cross-section from the Huangjiaping to Yinchang areas, showing the main litho-tectonic units, foliation attitudes and sample locations.

and *meta*-tuffaceous sandstone constitute the main rock types. Several serpentinized peridotite xenoliths within the basic-intermediate *meta*-volcanic interlayers are exposed within the feldspathic quartzite, quartz schist and quartzite (Fig. 3d). Emplacement of some later mafic dykes can also be observed (Fig. 3e). In the Yinchang area, the lithology changes to chlorite epidote schist, chlorite quartz schist, *meta*-tuff and silty phyllite (Fig. 3f).

The sampling points along this section focused on two outcrops of mafic *meta*-volcanics near the Dashanli region (Fig. 2b). The coordinates of the sampling points were concentrated at N32°41′52.71″, E105°08′43.02″ and N32°41′59.56″, E105° 08′37.67″. The sampled *meta*-volcanic rocks are mainly basaltic–basaltic andesitic, occurring in the form of layers in *meta*-sedimentary rocks such as feldspathic quartzite, quartz albite schist and quartz schist. The individual *meta*-volcanic layers outcrop with a width of one to several meters (Fig. 3a and b). The collected hand specimen samples are grey-green in color and have a compact massive to schistose structure (Fig. 3a–c). They show a scaly granular metamorphic texture and consist mainly of plagioclase (35–40 %), chlorite (35–40 %) and stilpnomelane (20 %), plus some ferro-titanium oxides (5 %) and a minimal amount of sericite particles (Fig. 3g–i). The dense massive structure coupled with the lack of terrigenous debris (such as quartz and other clay minerals) and the lack of remnant sedimentary texture confirm its nature as volcanic rocks (Bureau of Geology and Mineral Resources of Sichuan province, 1991). Chlorite occurs with anhedral to subhedral shapes. Many tiny minerals can be observed at the boundaries and interior of the chlorite grains, suggesting a certain degree of late alteration. Plagioclase is usually in the form of a subhedral plate, which generally has a 'dirty' surface and blurred grain boundary, indicating a late sodium alteration as well. Stilpnomelane is mainly in scaly or radial forms, and obvious pleochroism can be observed under the parallel polarizer. Ferro-titanium oxide exhibits opaque characteristics under the parallel and cross polarizers (Fig. 3g–i).

4. Analytical methods

Systematic zircon U–Pb geochronological, zircon Lu–Hf isotopic and whole-rock geochemical analyses were performed on the collected mafic *meta*-volcanic rock samples from the Bikou Terrane to obtain their recorded comprehensive information.

Zircon U–Pb analysis of samples 19BK-81 and 19BK-87 was conducted using a laser ablation-inductively coupled plasma-mass spectrometer (LA-ICP-MS) at the State Key Laboratory of Continental Dynamics at Northwest University in Xi'an, China. A Gatan MonoCL 3 + fluorescence spectrometer was used to obtain cathodoluminescence (CL) images of the selected crystals. During the analysis, a laser ablation spot size of approximately 24 μm and a frequency of 6 Hz were used. To correct for mass deviation and elemental fractionation, Harvard zircon 91,500 was employed as an external standard sample. The acquired data were calculated and plotted using Glitter 4.0 software from Macquarie

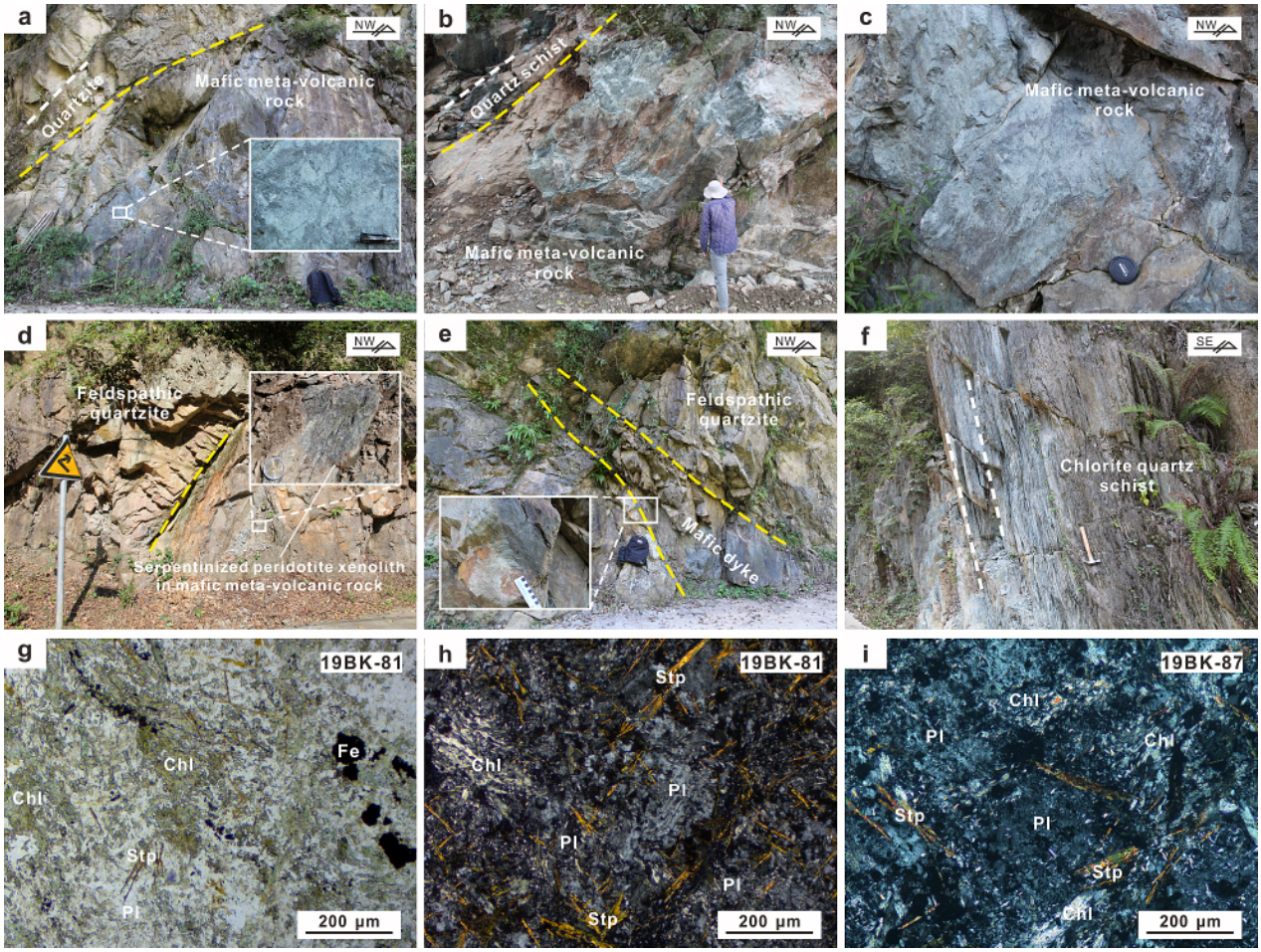

Fig. 3. Representative field photos from the Huangjiaping–Yinchang section and thin-section images of the mafic *meta*-volcanic samples. (a) Greyish-white quartzite with sampled grey-green mafic *meta*-volcanic rock interlayer, northern Huangjiaping area; (b) Well-developed greyish-white quartz schist and interlayered grey-green mafic *meta*-volcanic rock, southern Dashanli area; (c) Sampled grey-green mafic *meta*-volcanic rock in the south of Dashanli area; (d) Light-coloured feldspathic quartzite and interlayered grey-green sampled mafic *meta*-volcanic rock with serpentinized peridotite xenoliths, southern Dashanli area; (e) Mafic dyke intruded into feldspathic quartzite in the southern Yinchangli area, with distinct baking margins observable in feldspathic quartzite; (f) Grey-green chlorite quartz schist with a steep dip, Yinchang area; (g–i) thin-section images of the mafic *meta*-volcanic samples with visible minerals of plagioclase, chlorite, stilpnomelane and ferro-titanium oxide. Abbreviations: Chl, Chlorite; Fe, ferro-titanium oxide; Pl, Plagioclase; Stp, stilpnomelane. (For interpretation of the references to color in this figure legend, the reader is referred to the web version of this article.)

University, Australia, and ISOPLOT 3 (Ludwig, 2003). The $^{207}Pb/^{206}Pb$ age is used for grains older than 1000 Ma, while grains with an age younger than 1000 Ma adopt the $^{206}Pb/^{238}U$ age.

Zircon Lu–Hf isotope measurements were conducted using a MC-ICP-MS plus femto-second LA system at the Micro-Macro Geochemistry Technology (Langfang) Co., Ltd in China. Detailed analytical procedures and calibration methods are similar to those described by Wu et al. (2006). The isobaric interference of ^{176}Lu on ^{176}Hf was found to be negligible due to the significantly low $^{176}Lu/^{177}Hf$ ratio in zircon less than 0.002. The ε_{Hf} value was calculated by using each spot's dating age and the present chondritic $^{176}Hf/^{177}Hf$ ratio of 0.282785 and $^{76}Lu/^{177}Hf$ ratios of 0.0336 (Bouvier et al., 2008). The single-stage model age was determined in relation to a $^{176}Hf/^{177}Hf$ ratio of 0.28325 and a $^{176}Lu/^{177}Hf$ ratio of 0.0384 (Griffin et al., 2000), and the two-stage model age calculated using a $^{176}Lu/^{177}Hf$ ratio of 0.015 (Rudnick and Gao, 2014).

Whole-rock major and trace element geochemical analysis of sampled *meta*-volcanic rocks was carried out at the State Key Laboratory of Continental Dynamics, Northwest University in Xi'an, China, using X-ray fluorescence (XRF) and ICP-MS. The detailed method followed the procedure described in Liu et al. (2007). The accuracy of most elements analyzed was better than 5–10 % based on the analysis of standard samples.

5. Results

5.1. Zircon U–Pb ages

Two representative mafic *meta*-volcanic rock samples (19BK-81 and 19BK-87) were collected for zircon U–Pb dating. The detailed results are listed in Supplementary Table S1.

5.1.1. 19BK-81

Ninety spots from eighty-seven zircons were analyzed, of which seventy-six analyses are concordant within 93 and 109 percent. These are used in the following discussion. The dataset shows an age range from the Paleoarchean to Tonian (Fig. 4).

The Archean zircons mainly include three age groups: ca. 3.50, 2.88 and 2.72–2.62 Ga (Fig. 4c and d). Only one zircon grain with an age of ca. 3.50 Ga was found in sample 19BK-81. It exhibits a lath-like shape and a banded zoning internal zoning (Fig. 4a), indicative of a magmatic origin. Four spots with ages between ca. 3507 and 3502 Ma obtained from this grain show favorable consistency within the error range, demonstrating its Paleoarchean nature. The 2.88 Ga zircon grain is oval,

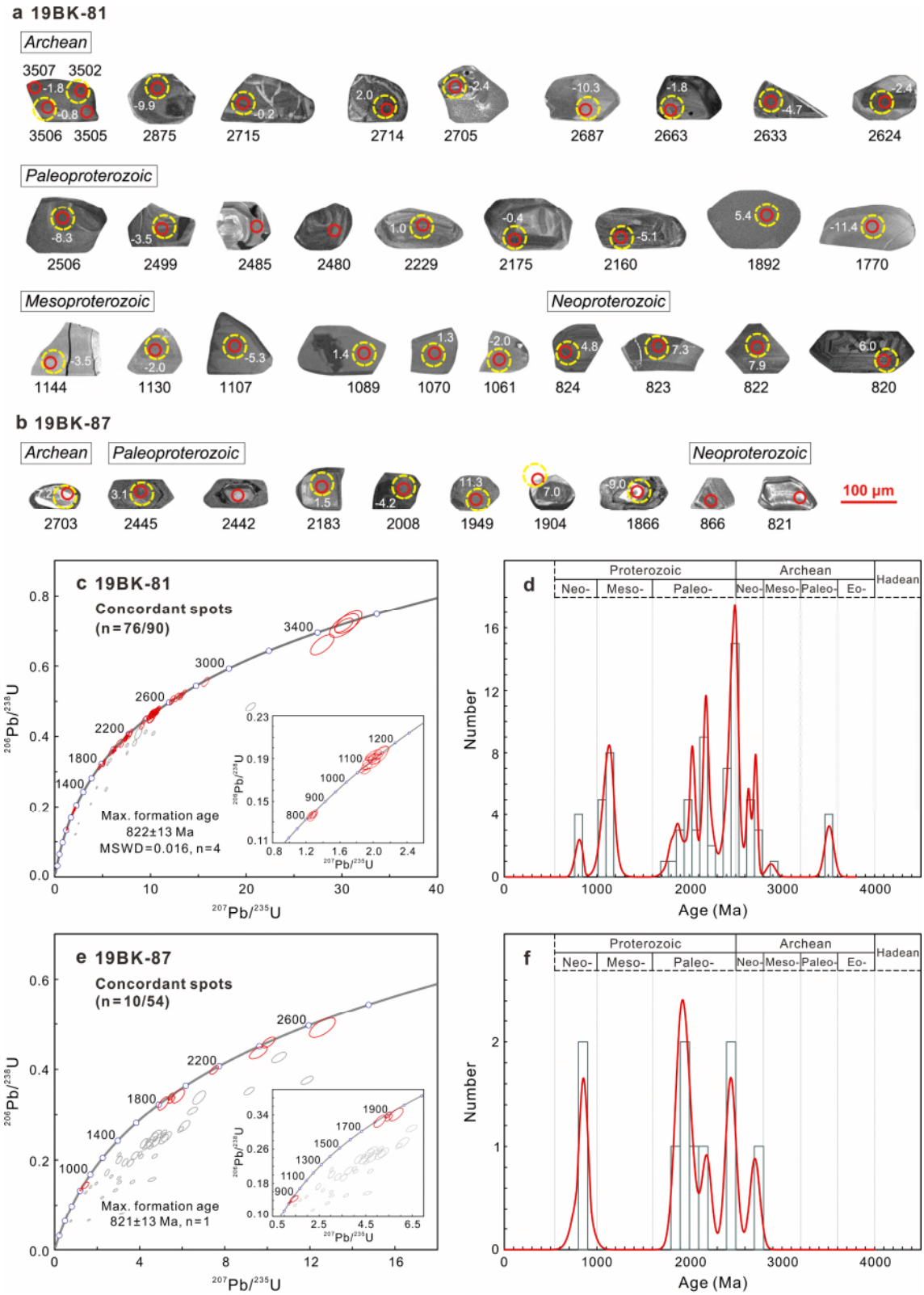

Fig. 4. (a)–(b) CL images of representative xenocrystic zircons. Solid red circles indicate the U–Pb analysis locations, while dashed yellow circles represent the Lu–Hf analysis locations. The black numbers indicate zircon ages (Ma), while the white numbers represent $\varepsilon_{Hf}(t)$ values. (c)–(f) Zircon U–Pb Concordia diagrams and age probability density distributions and curves of concordant zircons. Magenta ellipses represent concordant spots (90–110%), while grey ellipses indicate discordant spots. (For interpretation of the references to color in this figure legend, the reader is referred to the web version of this article.)

with a tiny inherited core and a wide-zonal growth rim (Fig. 4a). The higher Th/U ratio of 0.13 indicates it also belongs to a magmatic zircon (Fig. 5). Most of the 2.72–2.62 Ga grains exhibits a short prismatic shape with broad oscillating zoning in the core and a structureless rim (Fig. 4a). The total nine spots with Th/U ratios of 0.13–1.28 conducted on the magmatic core show ages ranging from ca. 2715 to 2624 Ma (Fig. 5).

The Paleoproterozoic ages account for the vast majority, including four age groups: ca. 2.52–2.37, 2.23–2.16, 2.07–1.95 and 1.89–1.77 Ga (Fig. 4c and d). The 2.52–2.37 Ga zircons are short prismatic and display typical magmatic oscillatory zoning patterns (Fig. 4a). The twenty-two spots have Th/U ratios higher than 0.08 and give ages ranging from ca. 2520 to 2371 Ma. The eleven concordant ages are obtained from the 2.23–2.16 Ga grains. Oscillatory zoning patterns (Fig. 4a) plus high Th/U ratios of 0.47–1.58 (Fig. 5) indicate they are of magmatic origin. Eight concordant zircons aged 2.07–1.95 Ga can be divided into two categories: one features a magmatic origin with oscillatory zoning and high Th/U (0.02–1.55) and the other has a metamorphic origin with structureless characteristics and low Th/U of 0.008 (Fig. 5). Minor 1.89–1.77 Ga zircons are long prismatic or oval shaped, with a broad oscillatory zoning or a uniform internal structure and varied Th/U ratios (0.07 and 0.24–1.06; Fig. 4a and 5). Five grains show ages from ca. 1892 to 1770 Ma.

The Mesoproterozoic zircons are limited to the latest Mesoproterozoic, concentrating on 1.16–1.05 Ga (Fig. 4c and d). These grains have a granular or short prism-like euhedral shape and show a relatively uniform internal structure with weak oscillatory zoning (Fig. 4a). Th/U ratios greater than 0.51 (Fig. 5) collectively indicate their derivation from mafic rocks. Thirteen effective ages obtained centered around ca. 1155 to 1054 Ma.

The youngest early Neoproterozoic ages were obtained from four zircons, yielding a mean weighted age of 822 ± 13 Ma (MSWD = 0.016) (Fig. 4c and d). Unfortunately, these zircons have euhedral and typical oscillatory zoning that developed typically in acidic rocks (Fig. 4a), indicating they were still xenocrystic zircons. Nevertheless, this also limits the maximum formation age of the sample 19BK-81 from another aspect, which is after ca. 822 Ma.

5.1.2. 19BK-87

Fifty-four zircons were extracted from sample 19BK-87, and fifty-four spots were analyzed on these grains. Unfortunately, most analyses show considerable discordances among their $^{207}Pb/^{206}Pb$, $^{207}Pb/^{235}U$ and $^{206}Pb/^{238}U$ ages (Fig. 4e and f). Such inconsistencies may be because of significantly later radioactive Pb-loss (Wu and Zheng, 2004). There are also minor measuring spots that have not recorded effective data due to the small size of zircons. Only ten results fall on the Concordia curve, with a concordance degree between 100 and 106 %. These data still include Archean, Paleoproterozoic and the youngest Tonian ages (Table S1; Fig. 4c and d).

Only one Archean zircon grain (ca. 2.70 Ga) shows a prismatic shape and has a typical magmatic internal oscillatory zoning internal structure (Fig. 4b). The high Th/U at 0.46 (Fig. 5) indicates that it should have crystallized in a magmatic event of ca. 2703 Ma.

The Paleoproterozoic ages also have four groups of ca. 2.44, 2.18, 2.01–1.95 and 1.90–1.87 Ga (Fig. 4e and f). The ca. 2.44 Ga zircons have a typical prismatic feature and exhibit a common inherited core with oscillatory zoning and a structureless metamorphic rim (Fig. 4b). The two ages obtained from the core are dated at ca. 2445 and 2442 Ma, alongside high Th/U ratios (0.71 and 0.60; Fig. 5), together indicating an early Paleoproterozoic magmatic event. The 2.18 and 2.01–1.95 Ga zircons are granular or prismatic. CL images show that the three grains with concordant ages have a core-rim structure (Fig. 4b). One age from a zircon core is ca. 2183 Ma (Th/U = 0.67), while two ages from two structureless zircons are ca. 2008 and 1949 Ma (Th/U = 0.01) (Fig. 5). A few 1.90–1.87 Ga zircons exhibit a similar morphology and internal structure to these of the 2.18–1.95 Ga grains (Fig. 4b). Two spots from the overgrowth rim and core gives ages of ca. 1904 Ma (Th/U = 0.01) and ca. 1866 Ma (Th/U = 0.04) (Fig. 5), respectively.

The two early Neoproterozoic ages were also obtained in sample 19BK-87 (Fig. 4e and f). Their CL images with strong luminescence and well-developed oscillatory zoning (Fig. 4b) are of typically acidic origin. One zircon grain of them is slightly older and yields an 866 ± 29 Ma age. The other one is younger, with an age of 821 ± 13 Ma, consistent with the youngest ages obtained from sample 19BK-81, indicating that the timing of sample 19BK-87 should be later than ca. 821 Ma.

Overall, the age groups of both samples can be summarized as ca.

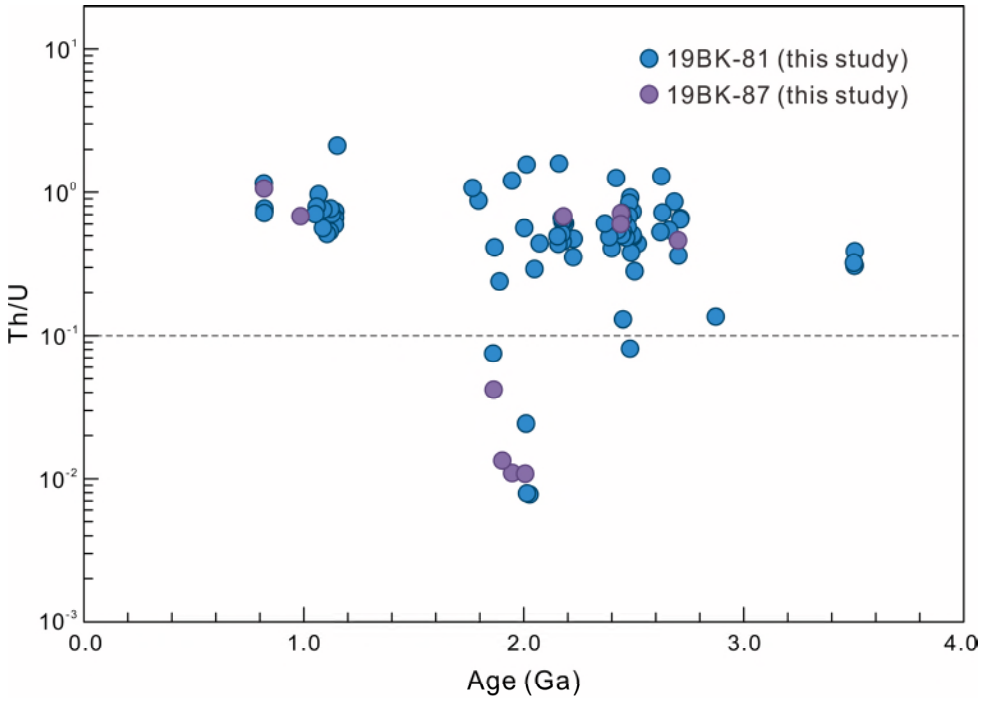

Fig. 5. Th/U ratio for each concordant zircon plotted against U–Pb age.

3.50, 2.88 and 2.72–2.62 Ga in the Archean, ca. 2.52–2.37, 2.23–2.16, 2.07–1.95 and 1.90–1.77 Ga in the Paleoproterozoic, ca. 1.16–1.05 Ga in the Mesoproterozoic, and ca. 820 Ma in the Neoproterozoic.

5.2. Hf isotopes

Indefinite points in samples 19BK-81 and 19BK-87 were selected for in-situ Lu–Hf isotope analysis. The detailed results can be found in Supplementary Table S2.

5.2.1. 19BK-81

A total of sixty-two Hf analyses were carried out on the zircons with concordant ages from sample 19BK-81 (Table S2). Among these, eleven results were concentrated on the Archean zircons. Two analyses from ca. 3.50 Ga zircon have negative $\varepsilon_{Hf}(t)$ of −0.8 and −1.8 plus ancient two-stage model (T_{DM2}) ages of 3.83 and 3.88 Ga (Fig. 6). One spot from ca. 2.88 Ga zircon shows $\varepsilon_{Hf}(t)$ of −9.9 and T_{DM2} age of 3.89 Ga. Eight results from ca. 2.72–2.62 Ga grains have corresponding $\varepsilon_{Hf}(t)$ and T_{DM2} ages vary from −10.3 to + 2.0 and 3.77 to 3.04 Ga, respectively (Fig. 6). Additionally, thirty-six results from the Paleoproterozoic grains possess $\varepsilon_{Hf}(t)$ and T_{DM2} ages expressed as: −17.7–+5.8 and 4.06–2.61 Ga (fifteen analyses) for the 2.52–2.37 Ga zircons, −16.1–+2.5 and 3.77–2.52 Ga (seventeen analyses) for the 2.23–1.95 Ga zircons, and −11.4–+5.4 and 3.16–2.20 Ga (four analyses) for the 1.89–1.77 Ga zircons (Fig. 6). Furthermore, eleven spots from the Mesoproterozoic (1.16–1.05 Ga) zircons show $\varepsilon_{Hf}(t)$ of −7.9 to + 1.6, with T_{DM2} ages ranging from 2.41 to 1.82 Ga (Fig. 6). Lastly, four Neoproterozoic zircons consistently yield positive $\varepsilon_{Hf}(t)$ of + 4.8–+7.9 and old T_{DM2} ages of 1.41–1.21 Ga (Fig. 6).

5.2.2. 19BK-87

Due to the age discordance of most zircons, only six spots of Hf isotope analysis were carried out on this sample (Table S2). The one Archean zircon (2.70 Ga) has a significantly positive $\varepsilon_{Hf}(t)$ of + 7.2, with a comparable T_{DM2} age of 2.72 Ga (Fig. 6). Out of the five results obtained from the Paleoproterozoic zircons, the $\varepsilon_{Hf}(t)$ and T_{DM2} ages of ca. 2.44 Ga zircon are + 3.1 and 2.77 Ga, whereas those of 2.18 Ga and 2.00 Ga zircons are −4.2 and + 1.5, and 2.88 Ga and 2.66 Ga. In addition, two spots from 1.90 Ga and 1.87 Ga zircons show $\varepsilon_{Hf}(t)$ of + 7.0 and −9.0 and T_{DM2} ages of 2.11 and 3.07 Ga (Fig. 6).

5.3. Major and trace elements

Representative mafic *meta*-volcanic rock samples for whole-rock geochemistry were collected from two points in the Dashanli area. The detailed results are listed in Supplementary Table S3.

Overall, the mafic *meta*-volcanic rock samples show a relatively consistent pattern, revealing that they were derived from a homogenous source and thus were combined to be discussed together in the subsequent discussion chapters. The mafic *meta*-volcanic rock samples are featured by a limited range of SiO_2 (46.95–54.36 wt%) (Table S3), belonging to basic-intermediate volcanics. These samples exhibit high TFe_2O_3 (11.48–15.67 wt%), Al_2O_3 (12.45–14.90 wt%), TiO_2 (2.43–3.16 wt%) and P_2O_5 (0.32–0.37 wt%), as well as low MgO (3.91–6.94 wt%) and CaO (3.42–4.87 wt%) (Table S3). They show low values of $Mg^{\#}$ (37.3–47.9), and significant variations for Ni (10.8–61.6 ppm), Cr (2.00–95.5 ppm) and V (288–460 ppm) (Table S3). Besides, these samples also exhibit varied Zr (198–351 ppm) and Hf (4.97–8.61 ppm) (Table S3). The low Nb/Y (0.60–0.77) and Zr/TiO_2 (67–139) ratios, plus high $Na_2O + K_2O$ (5.19–6.19) (Fig. 7a and b), imply that they have a composition similar to alkaline basalts and basaltic andesite (Winchester and Floyd, 1977). In addition, La, Hf, Nb and Th correlate positively with Zr variations (Fig. 7c and d).

In the chondrite-normalized rare earth element (REE) spider diagram (Fig. 8a), these mafic *meta*-volcanic rock samples exhibit a significant 'rightward' pattern of enrichment of light rare earth elements (LREEs) relative to heavy rare earth elements (HREEs), with $(La/Yb)_N$ ranging from 2.45 to 6.57. They show weak negative Eu anomalies, with Eu/Eu* ratios of 0.79 to 0.87. In the primitive mantle-normalized multi-element spider diagram (Fig. 8b), the samples have OIB-like trace-element patterns, which are, enriched in large ion lithophile elements (LILEs) such as Rb, Ba and Sr. Although they are enriched in high field strength elements (HFSEs) like Th, U, Nb, Ta and Ti than those of E-MORB- and arc-like volcanics in the Bikou Terrane (Fig. 8b), these rocks also show variable degrees of negative Nb and Ta anomalies.

6. Discussion

6.1. Origin of the mafic meta-volcanic rocks

A critical prerequisite for employing xenocrystic zircons extracted from the mafic *meta*-volcanic rocks in this study to investigate the deep crustal properties of the Bikou Terrane is to define the origin of the mafic volcanic rocks initially. This necessitates first determining the age and nature of the mafic rocks and confirming the presence of crustal contamination during the magma evolution.

6.1.1. Age of the mafic meta-volcanic rocks

The low silicon concentration in mafic rocks poses a challenge to forming saturated zircon crystals during the cooling and solidification of the parent magma (Hoskin and Schaltegger, 2003; Wu and Zheng, 2004). Nevertheless, some xenocrystic zircons can be incorporated into mafic rocks during rapid magma upwelling on the surface (Page et al., 2007; Stern et al., 2010). These zircons may originate from country rocks or from contamination (Belousova et al., 2002; Zheng et al., 2009; Lupulescu et al., 2023). This provides an opportunity to compensate for the difficulty in forming primary zircons in the mafic magma and to explore their formation age. By determining the age of the youngest captured zircons, in conjunction with regional geological evidence, it becomes possible to gain insights into the formation age of mafic rocks.

In this study, a significant number of zircons with the Archean to

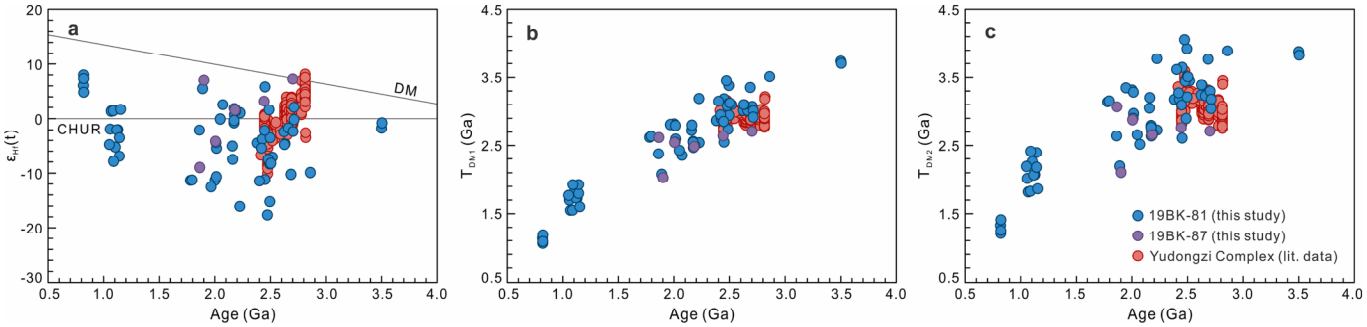

Fig. 6. Zircon U–Pb age versus $\varepsilon_{Hf}(t)$ (a), T_{DM1} (b) and T_{DM2} (c) diagrams. Literature data of the Yudongzi Complex are from Hui et al., (2017,2019), Zhou et al. (2018), Chen et al. (2019), Zhang et al. (2020) and Sun et al. (2022).

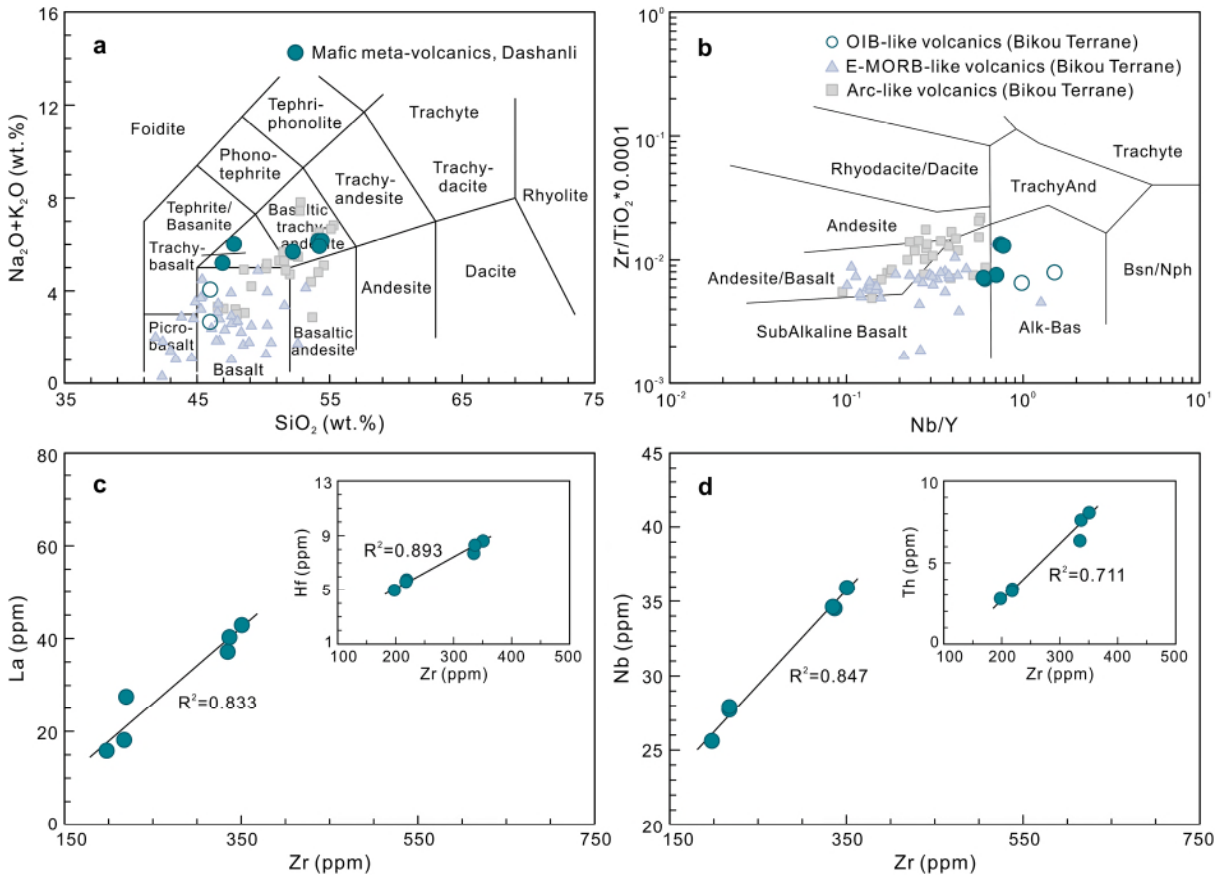

Fig. 7. (a) TAS diagram (Wilson, 1989); (b) Nb/Y versus Zr/TiO_2 diagram (Winchester and Floyd, 1977); (c) Zr versus La and Hf diagrams; (d) Zr versus Nb and Th diagrams. OIB-like volcanics (Wang et al., 2008), E-MORB-like volcanics (Xia et al., 1996, 2007; Xu et al., 2002; Yan et al., 2004a,b; Lai et al., 2007; Wang et al., 2008) and arc-like volcanics (Xia et al., 1996, 2007; Xu et al., 2002; Yan et al., 2004a,b; Wang et al., 2008) from the Bikou Terrane are shown for comparison.

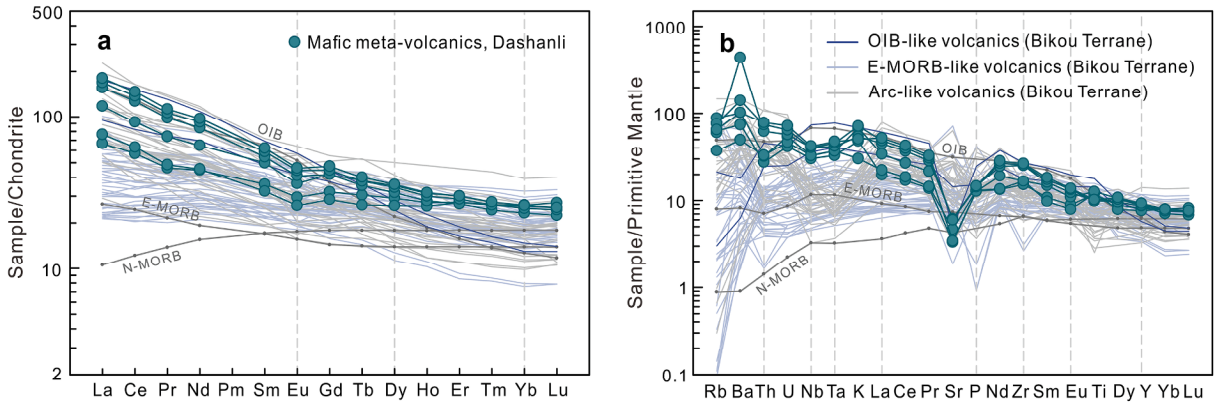

Fig. 8. Chondrite-normalized REE and primitive-mantle-normalized multi-elements diagrams. The normalizing chondrite, primitive mantle, OIB, E-MORB and N-MORB values are from Sun and McDonough (1989). Refer to Fig. 7 for other data sources.

Mesoproterozoic ages were found in the two samples, and most of these zircons exhibit typical oscillatory zoning (Fig. 4a and b), suggesting the presence of crustal components inherited during the evolution of the parent magma. The four youngest zircons in sample 19BK-81 yielded consistent ages within age errors, with a mean weighted age of 822 ± 13 Ma (Fig. 4c and d). In sample 19BK-87, although many ages are discordant, the similar youngest early Neoproterozoic age of 821 ± 13 Ma also appears (Fig. 4e and f). Unfortunately, all five zircons exhibit characteristics typical of zircons in acidic rocks in their CL images (Hoskin and Schaltegger, 2003), represented by the relatively narrow oscillatory zoning (Fig. 4a and b). This implies that these five zircons are still xenocrystic during the ascent of the magma. Nonetheless, this result helps establish a maximum age limit for the investigated samples in the Huangjiaping-Yinchang section, suggesting that the formation age of these *meta*-volcanics should be at least younger than approximately 820 Ma.

Spatial relationships in regional geological records can provide crucial constraints on the age of these *meta*-volcanic rocks. Existing research indicates that the basic-intermediate and acidic *meta*-volcanic rocks within the Bikou Group have consistent eruption ages, falling within the range of approximately 846 to 764 Ma (Zhao et al., 1990; Yan et al., 2003; Lai et al., 2007; Wang et al., 2008). The maximum

formation age of the mafic *meta*-volcanic rock samples in the Bikou Group, as determined from the Huangjiaping-Yinchang section in this study, aligns with the previously established formation time frame. This suggests that the samples under investigation likely fall within the age range after approximately 820 Ma but before the latest Tonian. Regional spatiotemporal relationships support this inference, including the presence of the Hengdan Group with a maximum depositional age of around 720 Ma, as well as the covered glacial-interglacial Cryogenian and carbonate platform Ediacaran strata (e.g., Hui et al., 2021c; Gu et al., 2023).

Therefore, this body of evidence from this study provides a systematic chain of support for the formation age of the mafic *meta*-volcanic rock samples within the Bikou Group. Specifically, they appear to have formed in the latest Tonian period, after approximately 820 Ma, and are likely consistent with the established age range of the Bikou Group.

6.1.2. *Nature of the mafic meta-volcanic rocks*

The mafic *meta*-volcanic rock samples investigated in this study show loss on ignition values ranging from 2.97 to 3.62 wt% (Table S3), which can be attributed to varying degrees of secondary alteration. The low greenschist facies metamorphism and substantial fluid alteration observed in the field and under the microscope further corroborate this observation (Fig. 3). Hydrothermal alteration and metamorphism typically lead to the mobilization of fluid-mobile elements, including major elements, as well as LILEs. HFSEs, REEs and transition elements tend to remain relatively immobile (Taylor and Mclennan, 1985; Polat and Hofmann, 2003). In the case of the *meta*-volcanic rock samples, the variations in La, Hf, Th and Nb relative to Zr reveal robust positive linear correlations (Fig. 7c and d). In contrast, those in Sc and Ni concerning Zr show strong negative correlations (not shown), suggesting that REEs, HFSEs and transition elements remained immobile during the secondary alteration and later metamorphism. Consequently, these elemental data are utilized to elucidate the processes of petrogenesis and tectonic setting further below.

The mafic *meta*-volcanic rock samples exhibit OIB-like REEs and trace-element patterns, suggesting they likely originated from a deep asthenospheric or lithospheric mantle source like OIB (Taylor and McLennan, 1985; Sun and McDonough, 1989; Zhao and Asimow, 2018). However, these rocks show distinctive features of LILEs enrichments and slight Nb and Ta depletion compared to the OIB pattern (Fig. 8). These variations can be attributed to the influence of crustal contamination or source enrichment. Considering this OIB-like *meta*-volcanic rocks do not exhibit distribution patterns similar to those of arc volcanic rocks within the Bikou Group (Fig. 8), it suggests that they may not originate from a mantle wedge source subjected to subduction-related assimilation (e.g., Zhao and Asimow, 2018; Zhao et al., 2019). Crustal contamination is a pivotal factor that significantly impacts the geochemical compositions of mafic rocks. Crustal material typically displays elemental traits characterized by high SiO_2, K, Na and LILEs, and low MgO. Conversely, they tend to have lower levels of HFSEs, notably Nb and Ta (Sun and McDonough, 1989; Rudnick and Gao, 2014). The incorporation of crustal materials, in particular, elevates the silica content and induces a shift in the trace-element patterns, resulting in apparent spikes of Nb and Ta but positive anomalies of Zr and Hf (e.g., Zhou et al., 2006; Zhao and Zhou, 2008). The basic-intermediate composition of *meta*-volcanic rocks in the Dashanli area in this study indicates that silica was likely to be added during the evolution of the mantle-derived magma (Fig. 7c and d), suggesting a possible degree of crustal involvement rather than the primitive mantle source's property. The slightly negative Nb and Ta plus relatively positive Zr and Hf anomalies in the primitive mantle-normalized elemental patterns reflect the contribution of the upper crustal contamination as well (Fig. 8b). Some trace element ratio

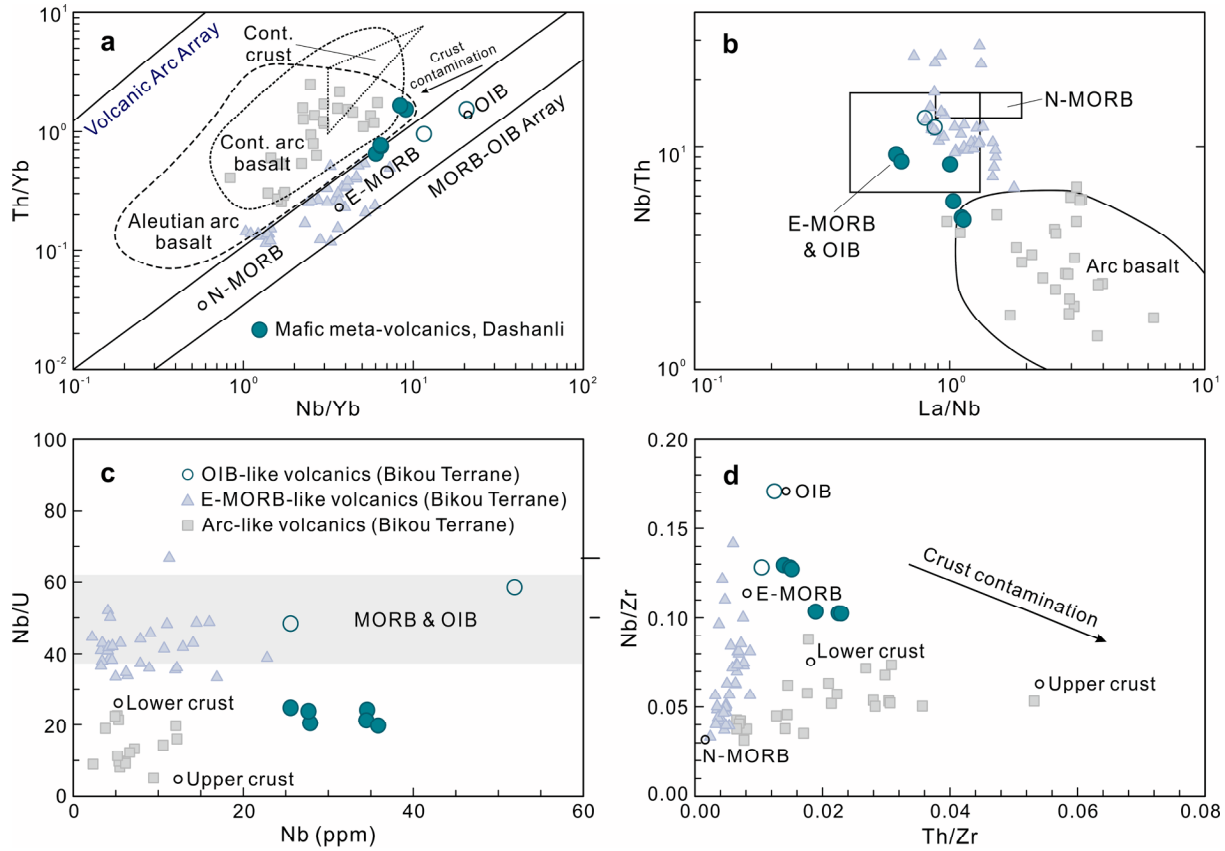

Fig. 9. (a) Nb/Yb versus Th/Yb diagram (Pearce, 2008); (b) La/Nb versus Nb/Th diagram (Zhang et al., 2012); (c) Nb versus Nb/U diagram; (d) Th/Zr versus Nb/Zr diagram. The normalizing OIB, E-MORB, N-MORB, lower crust and upper crust values are from Sun and McDonough (1989). Refer to Fig. 7 for other data sources.

features also support this conjecture. In the Nb/Yb versus Th/Yb binary diagram (Fig. 9a), these volcanic rock samples exhibit low Nb/Yb ratios (5.84–8.76) and Th/Yb ratios (0.63–1.82), showing an evolution trend from OIB-E-MORB to arc basalt (Pearce, 2008). Such a phenomenon can also be noticed through the covariation of La/Nb and Nb/Th ratios (Fig. 9b). Considering their relatively low Nb/U (19.8–24.0) and Nb/Zr (0.10–0/13) ratios (Fig. 9c and d), these features suggest the crustal contamination process during the magma evolution (Wilson, 1989; Ringwood, 1990; Brenan et al., 1994; Rudnick and Gao, 2014). Furthermore, in addition to geochemical characteristics, the presence of the xenocrystic zircon grains also provides evidence of crustal contamination taking place in the magma plumbing system (Fig. 4), since the hot melts derived from the mantle will inevitably assimilate country rocks (Zheng et al., 2009; Lupulescu et al., 2023). Therefore, we suggest that the mafic *meta*-volcanic rocks were sourced from a deep mantle similar to OIB, with crustal contamination playing a pivotal role in the magma's evolutionary process. The presence of OIB-like volcanic rocks which underwent crustal contamination on the other domain of the Bikou Terrane further supports the existence of a similar OIB-like mantle source (Wang et al., 2008).

Originating from the deep OIB-like mantle and marked by notable crustal contamination, the mafic *meta*-volcanic rocks are presumed to be formed within a tectonic setting associated with an intra-plate extension (Hui et al., 2021b, 2022a). In light of the geological context of the Bikou Group, which is believed to have been generated during a process involving subduction and concurrent back-arc extension (Hui et al., 2021b, 2022a), we contend that the suite of mafic *meta*-volcanic rocks examined in this study also owes its origins to a tectonic setting associated with a local extension occurring within the context of subduction. These shared pieces of evidence suggest that the OIB-like *meta*-volcanic rocks within the Bikou Group in the Huangjiaping-Yinchang section originated in situ within a localized back-arc extension setting during the late Tonian. The significant geochemical signatures of their crustal contamination further confirm that OIB-like magma interacted with the basement during magma upwelling and captured the xenocrystic zircons.

6.2. Existence of unexposed early Precambrian crust beneath the southern Bikou Terrane

The process of crustal contamination during the ascent of mafic magma provides vital insights into the deep crust (Stern et al., 2010; Woodhead et al., 2017; Shakerardakani et al., 2019; Gardiner et al., 2020). Given the absence of Paleoproterozoic–Mesoproterozoic sedimentary rocks within the Bikou Terrane, alongside the primarily prismatic zircon morphology, it is unlikely that the zircon xenocrysts found in the mafic *meta*-volcanic rocks of the Bikou Group in this study originated from recycled debris crystals in specific sedimentary rocks. Instead, they likely trace their origins to the unexposed basements of the Bikou Terrane (Zheng et al., 2009; Kostrovitsky et al., 2016). This inference allows us to better understand the Bikou Terrane by examining these valuable xenocrystic zircons from the mafic *meta*-volcanics.

The early Precambrian geological records exposed on the surface of the Bikou Terrane only include the northernmost Archean–Paleoproterozoic Yudongzi Complex (Hui et al., 2017, 2019). Whether the Bikou Terrane possesses a unified early Precambrian basement has remained a pivotal aspect of exploring its nature and evolutionary processes, primarily due to the limitations of basement distribution location and lack of recent research. As revealed in this study, the extensive collection of xenocrystic zircons extracted from the deep crust on the southern domain of the Bikou Terrane offers crucial evidence to address this inquiry. Overall, the exposed Yudongzi Complex documents four tectonic-thermal pulses: three in the Neoarchean (ca. 2.82–2.78, 2.70–2.63 and 2.52–2.45 Ga) (Hui et al., 2017, 2019; Zhou et al., 2018; Chen et al., 2019; Zhang et al., 2020) and one in the Paleoproterozoic (ca. 1.85 Ga) (Hui et al., 2017; Chen et al., 2019; Zhang et al., 2020). The ca. 2.82 Ga pulse is signified by the development of TTG gneiss with generally positive $\varepsilon_{Hf}(t)$ (+2.1 to + 8.1) and approaching T_{DM2} ages (3.10–2.80 Ga) (Fig. 6), as well as ca. 2.78 Ga plagioclase-hornblende schist with positive $\varepsilon_{Hf}(t)$ ranging from + 0.7 to + 6.9 and T_{DM2} ages ranging from 3.18 to 2.80 Ga (Sun et al., 2022), representing juvenile crust growth but experiencing nearly simultaneous reworking. The ca. 2.70–2.63 Ga pulse includes two categories: one with mostly depleted zircon Hf isotopes (−0.9 to + 3.9) and young T_{DM1} ages (3.01–2.83 Ga) (Fig. 6), characterized by amphibole plagiogneiss, indicating crustal growth and slight interaction between the mantle and preexisting crust (Hui et al., 2017); the other features varied Hf isotopes (−3.0 to + 3.9) and ancient T_{DM2} ages (3.32–2.90 Ga) (Fig. 6), marked by granitic gneiss, representing reworked ancient crust (Zhou et al., 2018; Chen et al., 2019). The ca. 2.52–2.45 Ga pulse is primarily identified by granitic gneiss with enriched to slightly depleted Hf isotopes (−10.1 to + 0.7) and ancient T_{DM2} ages (3.60–2.81 Ga) (Fig. 6), signifying the remelting of ancient crustal material (Hui et al., 2017, 2019; Zhou et al., 2018; Chen et al., 2019). In addition, the pulse at ca. 1.85 Ga represents a significant regional metamorphic event (Hui et al., 2017; Chen et al., 2019).

These four pulses have not only been documented by the Yudongzi Complex but are also prominently visible in the ages of xenocrystic zircons examined in this study. While the zircon xenocrysts dated in this study cover a range from the Mesoarchean to Mesoproterozoic, it's worth noting that several pulses match well with the episodic tectono-thermal events of the Yudongzi Complex (Fig. 6). The xenocrysts dated at around 2.72–2.62 Ga exhibit a diverse range of Hf isotope variations, from enriched to depleted (-10.3 to + 7.2), and T_{DM2} ages spanning from ancient to more nearing (3.77–2.72 Ga) (Table S2), closely overlapping the age population and magma nature those of the Yudongzi Complex (Hui et al., 2017; Zhou et al., 2018; Chen et al., 2019; Zhang et al., 2020). Similarly, a significant number of ca. 2.52–2.37 Ga zircon xenocrysts share characteristics of enriched to slightly depleted $\varepsilon_{Hf}(t)$ (-17.7 to + 5.8) and ancient T_{DM2} ages (4.06–2.61 Ga) (Table S2), covering the features of the ca. 2.52–2.45 Ga pulse recorded by the Yudongzi Complex as well (Hui et al., 2017, 2019; Zhou et al., 2018; Chen et al., 2019; Zhang et al., 2020). Moreover, the mafic *meta*-volcanic rock samples also exhibit a striking similarity in the presence of late Paleoproterozoic xenocrystic zircons from ca. 1.90–1.77 Ga. These distinctive characteristics are especially conspicuous in the binary diagram (Fig. 6), which clearly illustrates that the xenocrystic zircons obtained in this study contain zircons sharing Hf isotope characteristics akin to those of the Yudongzi Complex. In a comparative sense, these features indicate that the xenocrystic zircons from the mafic *meta*-volcanic rocks mainly retain and overlap the Archean–Paleoproterozoic tectono-thermal events carried by the Yudongzi Complex. More importantly, they also record more additional deep information than the Yudongzi Complex.

Therefore, we propose that an unexposed early Precambrian crust exists in the southern Bikou Terrane, which appears to have undergone episodic evolution similar to but not limited to that of the Yudongzi Complex. These further imply a unified and broader distribution of basements beneath the Bikou Terrane than previously thought. In addition to the information gained from the Yudongzi Complex, the unified crust might have undergone a more intricate evolution.

6.3. Paleoarchean to Mesoproterozoic crustal evolution of the northwestern Yangtze Block

The valuable dataset presented by the xenocrystic zircons in this study, serving as an exceptional complement to the Yudongzi and Houhe complexes, helps us to delve deeper into the early episodic crustal evolution in the northwestern Yangtze Block.

6.3.1. Paleo- to Neoarchean crustal components

Hints at the existence of crustal remnants as old as Paleoarchean are

suggested by the occurrence of Paleoarchean xenocrystic zircons (ca. 3.50 Ga) in this study, although they are found in only a tiny portion of the early Precambrian zircon xenocrysts in the mafic *meta*-volcanic rock samples (Fig. 4). The closed Hf isotopes to that of chondrite (-0.8 and −1.8) and the Eoarchean Hf model ages (T_{DM2} ages of 3.83 and 3.88 Ga) (Fig. 6) jointly indicate that there may be older Eoarchean components that shaped the northwestern Yangtze crust. Nevertheless, the relatively limited availability of objective zircons suggests that more research is needed to advance this inference.

The xenocrystic zircons provide evidence for two major pulses of crustal growth or reworking at ca. 2.88 Ga in the Mesoarchean and 2.72–2.62 Ga in the Neoarchean (Fig. 6). This counterpart of rocks of Meso- to Neoarchean ages have been identified in the Yudongzi Complex, including ca. 2.82 Ga TTG gneiss and ca. 2.78 Ga plagioclase-hornblende schist, and ca. 2.70–2.63 Ga amphibole plagiogneiss, TTG gneiss and granitic gneiss (Hui et al., 2017; Zhou et al., 2018; Chen et al., 2019; Zhang et al., 2020). It speculates the northwestern Yangtze Block might have experienced a juvenile crustal growth with involvement of both juvenile and ancient materials event at ca. 2.88–2.78 Ga and a subsequent ca. 2.72–2.62 Ga co-developed of new crustal growth and reworking of ancient crust in the Mesoarchean and Neoarchean, respectively.

6.3.2. Multiple Paleoproterozoic crustal reworking

The ca. 2.52–2.37, 2.23–2.16 and 2.07–1.95 Ga tectono-thermal events represent three major pulses of crustal reworking in the northwestern Yangtze Block. The associated evidence of ca. 2.52–2.37 Ga event was correspondingly identified from the xenocrystic zircons, as well as from the Yudongzi Complex (Hui et al., 2017, 2019; Zhou et al., 2018; Chen et al., 2019; Zhang et al., 2020). Xenocrystic zircons from the two studied samples form a major age group of ca. 2.52–2.37 Ga (Fig. 4). Most of them have negative $\varepsilon_{Hf}(t)$ (-17.7 to −2.2) with Eoarchean–Mesoarchean T_{DM2} ages (4.06–3.09 Ga) (Fig. 6), which demonstrates a dominant process of old continental crustal reworking into the early Paleoproterozoic magmas. The similar-aged igneous rocks are also preserved in the Yudongzi Complex, which also features mostly negative $\varepsilon_{Hf}(t)$ ranging from − 10.1 to + 0.7 and T_{DM2} ages from 3.60 to 2.81 Ga (Fig. 6). On the contrary, the xenocrystic zircons of this study dominantly delineated the 2.23–2.16 and 2.07–1.95 Ga events. Their negative to slightly positive $\varepsilon_{Hf}(t)$ (-16.1–+2.5) and Eoarchean–Neoarchean T_{DM2} ages (3.78–2.52 Ga) (Fig. 6) delineate a process predominantly of the reworking of ancient continental crustal components with minor juvenile additions. Corresponding crystalline rocks are merely documented in the Houhe Complex, i.e., the ca. 2.09–2.08 Ga grey gneisses (Wu et al., 2012; Deng et al., 2020). Some metamorphic zircons aged 2.07–1.95 Ga also record advanced metamorphism (Fig. 5). The clues highlight the three main recycling events in the early Paleoproterozoic.

Late Paleoproterozoic xenocrystic zircons are rare and constitute an age group ranging from ca. 1.90 to 1.77 Ga (Fig. 4). Like the pre-late Paleoproterozoic xenocrystic zircons, these zircons also have a typical magmatic broad oscillatory zoning or a uniform internal structure (Fig. 4). These xenocrystic zircons can be divided into two categories: one with positive $\varepsilon_{Hf}(t)$ (+7.0 and + 5.4) with and approaching T_{DM2} ages (2.11 and 2.20 Ga); the other features enriched Hf isotopes ($\varepsilon_{Hf}(t)$ = −11.4 – −2.1) and ancient T_{DM2} ages (3.14–2.64 Ga) (Fig. 6), suggestive of locally magma derivations from recycled ancient crustal components plus significant additions of juvenile materials in the late Paleoproterozoic. These are also clues of corresponding rock records, represented by the amphibolite with metamorphic ages at ca. 1.85 Ga in the Yudongzi Complex (Hui et al., 2017; Chen et al., 2019) and the ca. 1.76 Ga A-type granite in the Houhe Complex (Deng et al., 2020). The inference points to a predominant late Paleoproterozoic crustal reworking with crucial involvement of juvenile additions at ca. 1.90–1.76 Ga.

6.3.3. Imprint of latest Mesoproterozoic tectono-thermal activities

The xenocrystic zircons in this study first identify the late Mesoproterozoic tectono-thermal fingerprints in the northwestern Yangtze Block. The internal structures suggest that these zircon xenocrysts, with ages of approximately 1.16–1.05 Ga, exhibit a typical uniform pattern with weak oscillatory zoning features which prevail in the zircons from the basic-intermediate magma (Fig. 4). The negative to slightly positive $\varepsilon_{Hf}(t)$ (−7.9 to + 1.6) and Paleoproterozoic T_{DM2} ages (2.42 to 1.87 Ga) (Fig. 6) suggest a significant recycling plus new material involvement process during the latest Mesoproterozoic. Nevertheless, the current scarcity of related igneous rocks in the adjacent domain makes it challenging to accurately characterize the nature of the late Mesoproterozoic tectono-thermal events in the northwestern Yangtze Block.

Therefore, it is proposed that the northwestern Yangtze Block underwent several pulses of crustal evolution during the Paleoarchean to Mesoproterozoic, including a recycling event of Eoarchean crust at ca. 3.50 Ga, a dominant crustal growth event at ca. 2.88–2.78 Ga in the Mesoarchean, new crust growth/reworking events at ca. 2.72–2.62 Ga in the Neoarchean, episodes of reworking of ancient crust at ca. 2.52–2.37, 2.23–2.16 and 2.07–1.95 Ga. A further reworking event affecting ancient crust plus the addition of juvenile crust at ca. 1.90–1.76 Ga in the Paleoproterozoic, and a recycling event involving a new component at ca. 1.16–1.05 Ga in the latest Mesoproterozoic.

6.4. Comparison of early crustal evolution in the northern, northwestern and southwestern Yangtze Block

The critical xenocrystic zircon databases in this study, combined with records of Archean to Mesoproterozoic crystalline rocks in the Yangtze Block, enable us to re-evaluate the early crustal evolution within different domains (Fig. 10).

6.4.1. Discrete Archean crustal evolutionary history

Although more information needs to be extracted further, the discovery of the Paleoarchean zircon xenocrysts in this study enhances our comprehension of the early crust in the northwestern Yangtze margin at ca. 3.50 Ga. The Hf isotope findings indicate even more hints at the existence of crustal remnants as old as Eoarchean (Fig. 10). Traces of the Paleoarchean crustal components have also been identified from the northern Yangtze Block, which cover almost the entire Paleoarchean, including the ca. 3.45–3.43 Ga granitic gneiss (Guo et al., 2014a), ca. 3.31–3.29 Ga TTG gneiss (Gao et al., 2011; Guo et al., 2015), and ca. 3.26–3.22 Ga inherited zircons in the Kongling Complex (Gao et al., 2011; Guo et al., 2015). They mostly exhibit enriched zircon Hf isotopes, with their Hf model ages extending back to the Eo- to Paleoarchean (Fig. 10). The current scarcity of data leads us to posit that a Paleoarchean crustal reworking occurred in both the northern and northwestern Yangtze Block, and the initial continental crust growth might take place long before at the Eoarchean.

The Mesoarchean records tectono-thermal events have been documented within various domains (Fig. 10). In the northwest, it records a stage of juvenile crustal growth with involvement of both juvenile and ancient materials event at ca. 2.88–2.78 Ga. On the contrary, the northern and southwestern Yangtze Block preserves a wealth of more extensive and detailed information (Fig. 10). In the north, the Kongling Complex holds records of ca. 3.03–2.77 Ga TTG gneiss and granite (Zhang et al., 2006b; Gao et al., 2011; Chen et al., 2013b; Guo et al., 2015; Qiu et al., 2018), and ca. 2.95–2.76 Ga amphibolite and diabase (Wu et al., 2009; Peng et al., 2012; Li et al., 2014, 2018). The zircon Hf isotopic signatures indicate a significant recycling event with localized growth (Gao et al., 2011; Chen et al., 2013b; Li et al., 2014; Guo et al., 2015). This implication is further supported by the nature of ca. 2.90–2.86 Ga granite in the Zhongxiang Complex (Wang et al., 2018a; Wang et al., 2018b; Wang et al., 2018c). Nevertheless, the southwestern Yangtze Block features two episodes of ca. 3.11–3.06 and 2.92–2.85 Ga granitic magmatism with slightly positive $\varepsilon_{Hf}(t)$ values with approaching

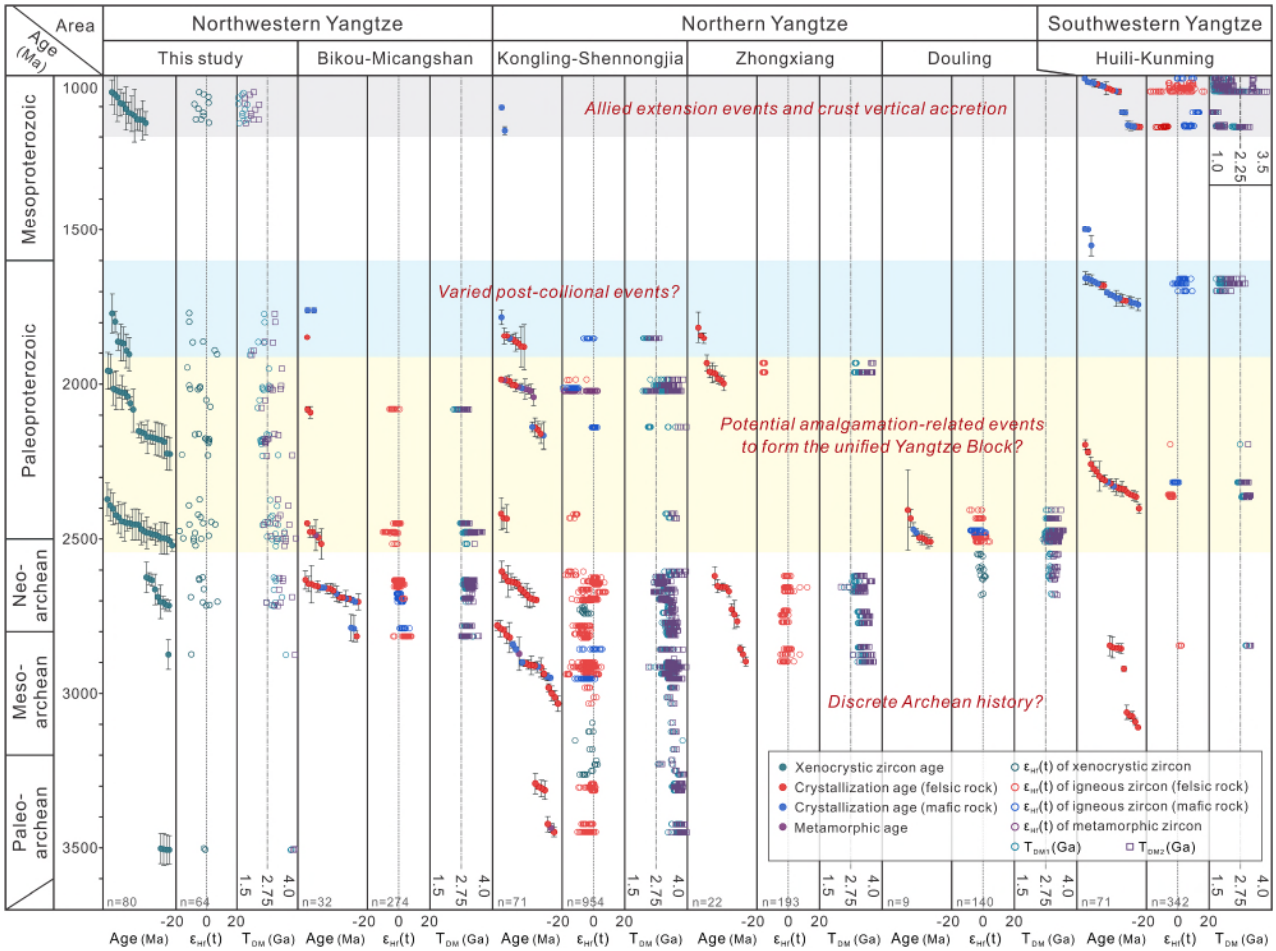

Fig. 10. A graphical comparison of zircon U–Pb ages, $\varepsilon_{Hf}(t)$, T_{DM1} and T_{DM2} database for Archean–Mesoproterozoic tectono-thermal events in the northwestern, northern and southwestern domains of the Yangtze Block. Data sources: Bikou-Micangshan region in the northwestern domain (Zhang et al., 2001, 2010; Wu et al., 2012; Hui et al., 2017, 2019; Zhou et al., 2018; Chen et al., 2019; Deng et al., 2020; Zhang et al., 2020; Sun et al., 2022); Kongling region in the northern domain (Zhang et al., 2006a; Zhang et al., 2006b; Zhang et al., 2006c; Xiong et al., 2008; Wu et al., 2009; Peng et al., 2012; Gao et al., 2011; Qiu et al., 2011, 2018; Wei and Jing, 2013; Chen et al., 2013b; Zhao, 2013; Yin et al., 2013; Li et al., 2014, 2018; Guo et al., 2014a, 2015; Du et al., 2016; Han et al., 2017, 2018, 2019; Han and Peng, 2020); Zhongxiang region in the northern domain (Zhang et al., 2011; Wang et al., 2013b, 2015, 2016, 2018a,b,c; Zhou et al., 2017; Wang and Dong, 2019); Douling region in the northern domain (Hu et al., 2013; Wu et al., 2014; Nie et al., 2016); Huili-Kunming region in the southwestern domain (Zhang et al., 2007; Geng et al., 2007; Greentree and Li, 2008; Guan et al., 2011; Zhao et al., 2010, 2020; Zhao and Zhou, 2011; Yang et al., 2012, 2016, 2023; Wang et al., 2013c, 2016, 2019; Zhu et al., 2016, 2017; Li et al., 2013a; Guo et al., 2014b; Chen et al., 2018, 2021; Cui et al., 2019, 2020, 2021; Lu et al., 2019; Liu et al., 2020, 2021; Shen et al., 2023). The spatiotemporal distribution can distinguish the model ages of mafic and felsic magmas. The annotated events of the Yangtze Block are derived from mainstream viewpoints (e.g., Cawood et al., 2020).

Hf model ages (Fig. 10), matching a remelting of juvenile crust process (Zhao et al., 2020; Cui et al., 2020, 2021; Yang et al., 2023). These delineate that during the Mesoarchean, the northern Yangtze underwent extended crustal reworking and modest growth from ca. 3.03 to 2.76 Ga. A crustal remelting event occurred in the southwest at around 3.11–2.85 Ga, while the northwestern domain saw a shorter juvenile crustal growth at 2.88–2.78 Ga.

The Neoarchean tectono-thermal events have had a substantial influence on the northwestern and northern Yangtze Block, while they remain undocumented in the igneous rocks of the southwestern region (Fig. 10). In the northwestern Yangtze Block, the period around 2.72–2.62 Ga witnessed the simultaneous development of new crust growth and reworking of the Paleo- to Mesoarchean crust (Hui et al., 2017). In the northern Yangtze Block, the varying Hf isotopes observed in A-type granites dated to approximately 2.70–2.61 Ga (Chen et al., 2013b; Guo et al., 2015) and 2.75–2.62 Ga (Zhou et al., 2015; Wang et al., 2013b, 2018a; Wang et al., 2018b; Wang et al., 2018c) in the Kongling and Zhongxiang complexes collectively indicate a substantial influx of new crustal components during the Neoarchean recycling of the lower crust. Thus, we propose that the northern and northwestern domains of the Yangtze Block likely experienced a combination of juvenile material formation and the reworking of the ancient crust during the ca. 2.72–2.62 Ga.

These clues indicate the northwestern and northern Yangtze may have entered coordinated evolution during the Neoarchean. This hints at the possibility of a discrete history between the northern-northwestern and southern Yangtze Block in the Neoarchean, though more research is required to evaluate this hypothesis (Cawood et al., 2020).

6.4.2. *Transformation and Paleoproterozoic crustal recycling*

The episodes of Paleoproterozoic tectono-thermal events have been demonstrated to represent major pulses of crustal reworking alongside juvenile additions, plus an advanced metamorphic event. The northern Yangtze Block also records Paleoproterozoic tectono-thermal imprints that are overlapping the four episodes of the northwestern Yangtze Block, represented by: 1) ca. 2.42 Ga granite (Guo et al., 2015), ca. 2.17–2.13 Ga I- and S-type granitoid and andesite (Han et al., 2018; Han and Peng, 2020), ca. 2.04–1.99 Ga I- and S- granitoid (Yin et al., 2013; Li

et al., 2014; Guo et al., 2015; Han et al., 2019) and ca. 1.88–1.78 Ga A-type granite and diabase (Xiong et al., 2008; Peng et al., 2012; Li et al., 2014; Han et al., 2019) in the Kongling Complex; 2) ca. 2.00–1.96 (Wang et al., 2015; Wang and Dong, 2019) and 1.85–1.82 Ga granite (Zhang et al., 2011; Zhou et al., 2017) in the Zhongxiang Complex; 3) ca. 2.51–2.41 Ga granitic gneiss and amphibole plagiogneiss (Hu et al., 2013; Wu et al., 2014; Nie et al., 2016) in the Douling Complex. The variable Hf isotope signatures (Fig. 10) indicate recycling of ancient continental crust in the early stage, and apparent crustal vertical accretion in the late stage. An obvious ca. 2.04–1.98 Ga high-grade metamorphism was also recorded in the Kongling Complex (Han et al., 2019; Liu et al., 2019). Nevertheless, the southwestern Yangtze Block features a prolonged crustal reworking process from approximately 2.40 to 2.20 Ga, supported by studies on granite in the Cuoke Complex (Wang et al., 2016; Cui et al., 2020; Liu et al., 2020; Yang et al., 2023). After a long gap, it underwent a predominant crustal growth at around 1.76–1.66 Ga, demonstrated by the predominately positive $\varepsilon_{Hf}(t)$ values with young Hf model ages (Fig. 10) from gabbro, diabase and basalt in the Dahongshan, Dongchuan, Tong'an and Hekou groups (Greentree and Li, 2008; Chen et al., 2013a; Lu et al., 2019; Fan et al., 2020; Shen et al., 2023). These characteristics indicate a clear shift in magmatism at ca. 1.90 Ga, whether in the north, northwest or southwest. This inference is additionally supported by the transition of granitoid from S-/I-types to A-type at ca. 1.90 Ga (Zhang et al., 2011; Li et al., 2014; Zhou et al., 2017), the concurrent occurrence of metamorphism at a similar age (Yin et al., 2013; Li et al., 2022) and the presence of volume extensional mafic magmatism after ca. 1.90 Ga (Peng et al., 2012; Li et al., 2014; Hui et al., 2017).

The transformation occurring at ca. 1.90 Ga aligns with inferences in recent years. The reworking of ancient crust, reflecting continuous craton stabilization associated with crustal thickening before ca. 1.90 Ga, is intricately connected to the global orogeny during the assembly of the Nuna (Columbia) supercontinent (e.g., Zhao et al., 2002, 2004; Wang et al., 2020). These orogenies contributed to welding discrete Archean terranes and their unification into the overall Yangtze Block (e.g., Zhao and Cawood, 2012; Cawood et al., 2020). Subsequently, the ensuing events are associated with an extensional setting related to the collapse or even the eventual break-up of the supercontinent (e.g., Meert and Santosh, 2017; Cawood et al., 2020).

6.4.3. *Comparable Mesoproterozoic magmatism*

The Yangtze Block transitioned into a relatively stable phase, marked by an extensional geological background, facilitating significant Mesoproterozoic sedimentation (Zhao and Cawood, 2012; Cawood et al., 2020). Especially in the late Mesoproterozoic, carbonate platform facies were documented on the northern and northwestern domains, while shallow-marine facies dominated the southwestern domain (Dong et al., 2024a; Dong et al., 2024b). In addition to sporadic and localized early Mesoproterozoic volcanic ash deposits in the southwest, comparable magmatic activity became apparent in the northern, northwestern and western regions (Fig. 10). In the north, it is primarily represented by ca. 1.18–1.10 Ga intercalated volcanic tuff within the Shennongjia Group's carbonate rocks (Qiu et al., 2011; Du et al., 2016). Pertinent records of magmatism in the northwest are exclusively found within the zircon xenocrysts detailed in this study (Fig. 10). The southwestern domain boasts notably magmatic records, giving rise to numerous granitic dykes and volcanic rock interlayers within the Kunyang and Huili groups (Zhu et al., 2016; Chen et al., 2018; Wang et al., 2019; Liu et al., 2021). Their Hf isotope signatures, ranging from enrichment to strong depletion (Fig. 10), chronicle a diverse array of events related to the vertical accretion of new crustal material toward the end of the Mesoproterozoic. These magmatic activities across the domains of the Yangtze Block are highly indicative of a regional extension at the latest Mesoproterozoic (Zhu et al., 2016; Chen et al., 2018; Wang et al., 2019).

7. Conclusion

Comprehensive zircon U–Pb geochronological, zircon Lu–Hf isotopic and whole-rock geochemical analyses of the mafic *meta*-volcanic rocks within the Bikou Group of the Bikou Terrane yield the following key conclusions:

(1) Geochronological data reported, coupled with analysis of internal structures, reveals that all extracted zircons are xenocrystic, with dispersed ages at approximately 3.50, 2.88 and 2.72–2.62 Ga in the Archean, about 2.52–2.37, 2.23–2.16, 2.07–1.95 and 1.90–1.77 Ga in the Paleoproterozoic, around 1.16–1.05 Ga in the Mesoproterozoic, and roughly 820 Ma in the Neoproterozoic.
(2) The youngest zircon age clusters, along with regional spatio-temporal relationships, suggest the mafic *meta*-volcanic rocks of the Bikou Group were mostly likely formed in the latest Tonian, after approximately 820 Ma.
(3) Geochemical analysis reveals characteristics of the mafic magma similar to OIB but show evident negative spikes in HFSEs such as Nb-Ta. This indicates that they were formed in a back-arc extensional setting and experienced substantial crustal contamination, confirming the inference that the xenocrystic zircons originate from the deep-seated continental crust.
(4) The combination of Hf isotopic analysis indicates that the vital information of the xenocrystic zircons is closely aligned with the Yudongzi Complex, implying a unified deep crust beneath the Bikou Terrane. However, imprints beyond the Yudongzi Complex indicate a more complex Archean to Mesoproterozoic crust composition and evolution.
(5) Examining the crustal evolution in the northwestern Yangtze Block reveals intermittent crustal growth/reworking from ca. 3.50 to 2.72 Ga in the Archean and ancient crust reworking plus late advanced metamorphism at ca. 2.52–1.95 Ga in the early Paleoproterozoic, followed by crust recycling plus critical vertical accretion at ca. 1.90–1.76 and 1.16–1.05 Ga in the latest Paleo- and Mesoproterozoic

CRediT authorship contribution statement

Bo Hui: Data curation, Formal analysis, Investigation, Writing – original draft. **Yunpeng Dong:** Conceptualization, Investigation, Supervision, Writing – review & editing. **Hongjun Qu:** Investigation, Supervision, Writing – review & editing. **Shengsi Sun:** Writing – review & editing. **Franz Neubauer:** Writing – review & editing. **Feifei Zhang:** Writing – review & editing. **Rutao Zang:** Formal analysis. **Shuxuan Yan:** Formal analysis, Resources. **Guiyun Wang:** Formal analysis, Resources.

Declaration of competing interest

The authors declare that they have no known competing financial interests or personal relationships that could have appeared to influence the work reported in this paper.

Data availability

Data will be made available on request.

Acknowledgments

We are grateful to Dr. Lei Yang from Northwest University for his assistance in the field. Financial support for this study was jointly provided by the National Natural Science Foundation of China (Grants: 42330310, 42202235, 41930217 and 41872236), the Young Talent Fund of Association for Science and Technology in Xi'an (Grant: 959202313087), the China Postdoctoral Science Foundation Funded

Project (Grant: 2021M702645), the Natural Science Basic Research Program of Shaanxi, China (Grant: 2022JQ-226), the Youth Innovation Team of Shaanxi Universities, and the MOST Special Fund from the State Key Laboratory of Continental Dynamics, Northwest University. Two reviewers are highly appreciated for their constructive reviews of the manuscript. Editor-in-Chief Prof. Jian Zhang are also thanked for the expeditious editorial handling.

Appendix A. Supplementary data

Supplementary data to this article can be found online at https://doi.org/10.1016/j.precamres.2024.107327.

References

Belousova, E., Griffin, W., O'Reilly, S.Y., Fisher, N., 2002. Igneous zircon: Trace element composition as an indicator of source rock type. Contrib. Miner. Petrol. 143 (5), 602–622.

BGMRSC, 1991. Bureau of Geology and Mineral Resources of Sichuan Province. In: Regional Geology of Sichuan Province. Geological Publishing House, Beijing, pp. 1–690.

Bouvier, A., Vervoort, J.D., Patchett, P.J., 2008. The Lu–Hf and Sm–Nd isotopic composition of CHUR: constraints from unequilibrated chondrites and implications for the bulk composition of terrestrial planets. Earth Planet. Sci. Lett. 273, 48–57.

Brenan, J.M., Shaw, H.F., Phinney, D.L., Ryerson, F.J., 1994. Rutile–aqueous fluid partitioning of Nb, Ta, Hf, Zr, U, and Th: implications for high field strength element depletions in island–arc basalts. Earth Planet. Sci. Lett. 128 (3–4), 327–339.

Cawood, P.A., Wang, W., Zhao, T.Y., Xu, Y.J., Mulder, J.A., Pisarevsky, S.A., Zhang, L.M., Gan, C.S., He, H.Y., Liu, H.C., Qi, L., Wang, Y.J., Yao, J.L., Zhao, G.C., Zhou, M.F., Zi, J.W., 2020. Deconstructing South China and consequences for reconstructing Nuna and Rodinia. Earth Sci. Rev. 204, 103–169.

Chaudhuri, T., Wan, Y., Mazumder, R., Ma, M., Liu, D., 2018. Evidence of enriched, Hadean mantle reservoir from 4.2-4.0 Ga zircon xenocrysts from Paleoarchean TTGs of the Singhbhum Craton, Eastern India. Sci. Rep. 8 (1), 7069.

Chen, F.L., Cui, X.Z., Lin, S.F., Wang, J., Yang, X.M., Ren, G.M., Pang, W.H., 2021. The 1.14 Ga mafic intrusions in the SW Yangtze Block, South China: Records of late Mesoproterozoic intraplate magmatism. J. Asian Earth Sci. 205, 104603.

Chen, K., Gao, S., Wu, Y.B., Guo, J.L., Hu, Z.C., Liu, Y.S., Zong, K.Q., Liang, Z.W., Geng, X.L., 2013b. 2.6-2.7 Ga crustal growth in Yangtze craton. South China. Precambr. Res. 224, 472–490.

Chen, W.T., Sun, W.H., Zhou, M.F., Wang, W., 2018. Ca. 1050 Ma intra-continental rift-related A-type felsic rocks in the southwestern Yangtze Block. South China. Precambr. Res. 309, 22–44.

Chen, Q., Sun, M., Zhao, G.C., Zhao, J.H., Zhu, W.L., Long, X.P., Wang, J., 2019. Episodic crustal growth and reworking of the Yudongzi terrane, South China: Constraints from the Archean TTGs and potassic granites and Paleoproterozoic amphibolites. Lithos 326, 1–18.

Chen, W.T., Zhou, M.F., Zhao, X.F., 2013a. Late Paleoproterozoic sedimentary and mafic rocks in the Hekou area, SW China: Implication for the reconstruction of the Yangtze Block in Columbia. Precambr. Res. 231, 61–77.

Condie, K.C., Bickford, M.E., Aster, R.C., Belousova, E., Scholl, D.W., 2011. Episodic zircon ages, Hf isotopic composition, and the preservation rate of continental crust. Geol. Soc. Am. Bull. 123 (5–6), 951–957.

Cui, X.Z., Wang, J., Sun, Z.M., Wang, W., Deng, Q., Ren, G.M., Liao, S.Y., Huang, M.D., Chen, F.L., Ren, F., 2019. Early Paleoproterozoic (ca. 2.36 Ga) post-collisional granitoids in Yunnan, SW China: Implications for linkage between Yangtze and Laurentia in the Columbia supercontinent. J. Asian Earth Sci. 169, 308–322.

Cui, X.Z., Wang, J., Ren, G.M., Deng, Q., Sun, Z.M., Ren, F., Chen, F.L., 2020. Paleoproterozoic tectonic evolution of the Yangtze Block: New evidence from ca. 2.36 to 2.22 Ga magmatism and 1.96 Ga metamorphism in the Cuoke complex, SW China. Precambr. Res. 337, 105525.

Cui, X.Z., Wang, J., Wang, X.C., Wilde, S.A., Ren, G.M., Li, S.J., Deng, Q., Ren, F., Liu, J. P., 2021. Early crustal evolution of the Yangtze Block: Constraints from zircon U-Pb-Hf isotope systematics of 3.1–1.9 Ga granitoids in the Cuoke Complex, SW China. Precambr. Res. 357, 106155.

Deng, Q., Wang, Z.J., Ren, G.M., Cui, X.Z., Cao, H.W., Ning, K.B., Ren, F., 2020. Identification of the ~2.09 Ga and ~1.76 Ga Granitoids in the Northwestern Yangtze Block: Records of the Assembly and Break-Up of Columbia Supercontinent. Earth Sci. 45, 3295–3312 in Chinese with an English abstract.

Dong, Y.P., Liu, X.M., Santosh, M., Zhang, X.N., Chen, Q., Yang, C., Yang, Z., 2011. Neoproterozoic subduction tectonics of the northwestern Yangtze Block in South China: Constrains from zircon U-Pb geochronology and geochemistry of mafic intrusions in the Hannan Massif. Precambr. Res. 189, 66–90.

Dong, Y.P., Liu, X.M., Santosh, M., Chen, Q., Zhang, X.N., Li, W., He, D.F., Zhang, G.W., 2012. Neoproterozoic accretionary tectonics along the northwestern margin of the Yangtze Block, China: constraints from zircon U-Pb geochronology and geochemistry. Precambr. Res. 196–197, 247–274.

Dong, Y.P., Sun, S.S., Yang, Z., Liu, X.M., Zhang, F.F., Li, W., Cheng, B., He, D.F., Zhang, G.W., 2017. Neoproterozoic subduction-accretionary tectonics of the South Qinling Belt. China. Precambr. Res. 293, 73–90.

Dong, Y.P., Sun, S.S., Santosh, M., Zhao, J., Sun, J.P., He, D.F., Shi, X.H., Hui, B., Cheng, C., Zhang, G.W., 2021. Central China Orogenic Belt and amalgamation of East Asian continents. Gondwana Res. 100, 131–194.

Dong, Y.P., Sun, S.S., Santosh, M., Hui, B., Sun, J.P., Zhang, F.F., Cheng, B., Yang, Z., Shi, X.H., He, D.F., Yang, L., 2022. Cross Orogenic Belts in Central China: Implications for the tectonic and paleogeographic evolution of the East Asian continental collage. Gondwana Res. 109, 18–88.

Dong, Y.P., Hui, B., Sun, S.S., He, D.F., Sun, J.P., Zhang, F.F., Cheng, C., Yang, Z., Shi, X. H., Zang, R.T., Long, X.P., Zhang, G.W., 2024a. Neoproterozoic tectonic evolution and proto-basin of the Yangtze Block. Earth Sci. Rev. under review, China.

Dong, Y.P., Hui, B., Sun, S.S., Sun, J.P., Zang, R.T., Zhang, B., Luo, Q.X., Chong, F.B., Yu, K.C., Fan, M.P., Li, Y.X., Li, Y.C., Zhu, X., Dai, Q.W., Zuo, Z.S., 2024b. The links between Neoproterozoic tectonics, paleoenvironment and Cambrian explosion in the Yangtze Block. China. Earth Sci. Rev. 248, 104638.

Du, Q.D., Wang, Z.J., Wang, J., Deng, Q., Yang, F., 2016. Geochronology and geochemistry of tuff beds from the Shicaohe Formation of Shennongjia Group and tectonic evolution in the northern Yangtze Block. South China. Int. J. Earth Sci. 105, 521–535.

Fan, H.P., Zhu, W.G., Li, Z.X., Zhong, H., Bai, Z.J., He, D.F., Chen, C.J., Cao, C.Y., 2013. Ca. 1.5 Ga mafic magmatism in South China during the break-up of the supercontinent Nuna/ Columbia: The Zhuqing Fe-Ti-V oxide ore-bearing mafic intrusions in western Yangtze Block. Lithos 168–169 (2), 85–98.

Fan, H.P., Zhu, W.G., Li, Z.X., 2020. Paleo-to Mesoproterozoic magmatic and tectonic evolution of the southwestern Yangtze Block, south China: New constraints from ca. 1.7–1.5 Ga mafic rocks in the Huili-Dongchuan area. Gondwana Res. 87, 248–262.

Gao, S., Ling, W.L., Qiu, Y.M., Zhou, L., Hartmann, G., Simon, K., 1999. Contrasting geochemical and Sm–Nd isotopic compositions of Archean metasediments from the Kongling highgrade terrain of the Yangtze Craton: Evidence for cratonic evolution and redistribution of REE during crust anatexis. Geochim. Cosmochim. Acta 63, 2071–2088.

Gao, S., Yang, J., Zhou, L., Li, M., Hu, Z.C., Guo, J.L., Yuan, H.L., Gong, H.J., Xiao, G.Q., Wei, J.Q., 2011. Age and growth of the Archean Kongling terrain, South China, with emphasis on 3.3 Ga granitoid gneisses. Am. J. Sci. 311, 153–182.

Gardiner, N.J., Kirkland, C.L., Hollis, J.A., Cawood, P.A., Nebel, O., Szilas, K., Yakymchuk, C., 2020. North Atlantic Craton architecture revealed by kimberlite hosted crustal zircons. Earth Planet. Sci. Lett. 534, 116091.

Geng, Y.S., Yang, C.H., Du, L.L., Wang, X.S., Ren, L.D., Zhou, X.W., 2007. Chronology and tectonic environment of the Tianbaoshan Formation: new evidence from zircon SHRIMP U-Pb age and geochemistry. Geol. Rev. 53, 556–563 in Chinese with an English abstract.

Geng, Y.S., Kuang, H.W., Liu, Y.Q., Du, L.L., 2017. Subdivision and correlation of the Mesoproterozoic stratigraphy in the western and northern margins of Yangtze block. Acta Geol. Sin. 91, 2151–2174 in Chinese with an English abstract.

Greentree, M.R., Li, Z.X., 2008. The oldest known rocks in south-western China: SHRIMP U-Pb magmatic crystallization age and detrital provenance analysis of the Paleoproterozoic Dahongshan Group. J. Asian Earth Sci. 33, 289–302.

Griffin, W.L., Pearson, N.J., Belousova, E., Jackson, S.E., Van Achterbergh, E., O'Reilly, S.Y., Shee, S.R., 2000. The Hf isotope composition of cratonic mantle: LAM-MC-ICPMS analysis of zircon megacrysts in kimberlites. Geochim. Cosmochim. Acta 64, 133–147.

Gu, Z.D., Jian, X., Liu, G.X., Shen, X.T., Fu, H.J., Zhai, X.F., Jiang, H., 2023. Age, provenance and tectonic setting of the Tonian-Cryogenian clastic successions in the northwest Bikou terrane, NW Yangtze Block. Central China. Precambr. Res. 397, 107197.

Guan, J.L., Zheng, L.L., Lui, J.H., Sun, Z.M., Cheng, W.H., 2011. Zircons SHRIMP U-Pb dating of diabase from Hekou, Sichuan Province, China and its geological significance. Acta Geol. Sini. 85 (4), 482–490 in Chinese with an English abstract.

Guo, J.L., Gao, S., Wu, Y.B., Li, M., Chen, K., Hu, Z.C., Liang, Z.W., Liu, Y.S., Zhou, L., Zong, K.Q., Zhang, W., Chen, H.H., 2014a. 3.45 Ga granitic gneisses from the Yangtze Craton, South China: Implications for Early Archean crustal growth. Precambrian Res. 242, 82–95.

Guo, Y., Wang, S.W., Sun, X.M., Wang, Z.Z., Yang, B., Liao, Z.W., Zhou, B.G., Jiang, X.F., Hou, L., Yang, B., 2014b. The Paleoproterozoic breakup event in the southwest Yangtze block: evidence from U-Pb zircon age and geochemistry of diabase in Wuding, Yunnan Province. SW China. Acta Geol. Sin. 88 (9), 1651–1665 in Chinese with an English abstract.

Guo, J.L., Wu, Y.B., Gao, S., Jin, Z.M., Zong, K.Q., Hu, Z.C., Chen, K., Chen, H.H., Liu, Y. S., 2015. Episodic Paleoarchean-Paleoproterozoic (3.3-2.0 Ga) granitoid magmatism in Yangtze Craton, South China: implications for late Archean tectonics. Precambr. Res. 270, 246–266.

Han, Q.S., Peng, S.B., Kusky, T.M., Polat, A., Jiang, X.F., Cen, Y., Liu, S.F., Deng, H., 2017. A Paleoproterozoic ophiolitic mélange, Yangtze Craton, South China: evidence for Paleoproterozoic suturing and microcontinent amalgamation. Precambr. Res. 293, 13–38.

Han, Q.S., Peng, S.B., Polat, A., Kusky, T., Deng, H., Wu, T.Y., 2018. A ca. 2.1 Ga Andean-type margin built on metasomatized lithosphere in the northern Yangtze Craton, China: Evidence from high-Mg basalts and andesites. Precambr. Res. 309, 309–324.

Han, Q.S., Peng, S.B., Polat, A., Kusky, T.M., 2019. Petrogenesis and geochronology of Paleoproterozoic magmatic rocks in the Kongling complex: evidence for a collisional orogenic event in the Yangtze craton. Lithos 342–343, 513–529.

Han, Q.S., Peng, S.B., 2020. Paleoproterozoic subduction within the Yangtze Craton: Constraints from Nb-enriched mafic dikes in the Kongling complex. Precambr. Res. 340, 105634.

Hawkesworth, C.J., Cawood, P.A., Dhuime, B., Kemp, T.I., 2017. Earth's continental lithosphere through time. Ann. Revi. Earth Plan. Sci. 45, 169–198.

He, S., Dong, Y.P., Zhang, F.F., Sun, S.S., Hui, B., He, W.D., 2022. Petrogenesis and tectonic implications of the late Neoproterozoic mafic dykes in the South Qinling Belt. China. Precambr. Res. 373, 106647.
Hoffman, P.F., 1989. Speculations on Laurentia's first gigayear (2.0 to 1.0 Ga). Geology 17 (2), 135–138.
Hoskin, P.W.O., Schaltegger, U., 2003. The composition of zircon and igneous and metamorphic petrogenesis. Rev. Mineral. Geochem. 53, 27–62.
Hu, J., Liu, X.C., Chen, L.Y., Qu, W., Li, H.K., Geng, J.Z., 2013. A ~2.5 Ga magmatic event at the northern margin of the Yangtze craton: Evidence from U-Pb dating and Hf isotope analysis of zircons from the Douling Complex in the South Qinling orogen. Chin. Sci. Bull. 58, 3564–3579.
Hui, B., Dong, Y.P., Cheng, C., Long, X.P., Liu, X.M., Yang, Z., Sun, S.S., Zhang, F., Varga, J., 2017. Zircon U-Pb chronology, Hf isotope analysis and whole-rock geochemistry for the Neoarchean-Paleoproterozoic Yudongzi complex, northwestern margin of the Yangtze craton. China. Precambr. Res. 301, 65–85.
Hui, B., Dong, Y.P., Zhang, F.F., Sun, S.S., Liu, X.M., Cheng, C., He, D.F., 2019. Geochronology and geochemistry of ca. 2.48 Ga granitoid gneisses from the Yudongzi Complex in the northwestern Yangtze Block. China. Geol. J. 54, 879–896.
Hui, B., Dong, Y.P., Liu, G., Zhao, H., Sun, S.S., Zhang, F.F., Liu, X.M., 2020. Origin of mafic intrusions in the Micangshan Massif, Central China: Implications for the Neoproterozoic tectonic evolution of the northwestern Yangtze Block. J. Asian Earth Sci. 190, 104132.
Hui, B., Dong, Y.P., Franz, N., He, S., 2021a. Detrital zircon U-Pb ages of metasedimentary rocks from the Neoproterozoic Zhoutan Group in the northern Cathaysia Block (South China): Provenance and tectonic implications. Int. Geol. Rev. 63 (9), 1132–1152.
Hui, B., Dong, Y.P., Zhang, F.F., Sun, S.S., He, S., 2021b. Petrogenesis and tectonic implications of the Neoproterozoic mafic intrusions in the Bikou Terrane along the northwestern margin of the Yangtze Block. South China. Ore Geol. Rev. 131, 104014.
Hui, B., Dong, Y.P., Zhang, F.F., Sun, S.S., He, S., 2021c. Neoproterozoic active margin in the northwestern Yangtze Block, South China: new clues from detrital zircon U-Pb geochronology and geochemistry of sedimentary rocks from the Hengdan Group. Geol. Mag. 158, 842–858.
Hui, B., Dong, Y.P., Zhang, F.F., Sun, S.S., Franz, N., He, D.F., He, S., 2022a. Geochronology, geochemistry, and isotopic composition of the early Neoproterozoic granitoids in the Bikou Terrane along the northwestern margin of the Yangtze Block, South China: Petrogenesis and tectonic implications. Precambr. Res. 377, 106724.
Hui, B., Dong, Y.P., Sun, S.S., Sun, J.P., Zhang, F.F., He, D.F., Li, Y.X., 2022b. Neoproterozoic tectonic evolution of the northern margin of the Yangtze plate: constraints from magmatic events. Acta Geol. Sin. 96 (9), 3034–3050 in Chinese with an English abstract.
Kemp, A.I.S., Wilde, S.A., Hawkesworth, C.J., Coath, C.D., Nemchin, A., Pidgeon, R.T., Vervoort, J.D., DuFrane, S.A., 2010. Hadean crustal evolution revisited: new constraints from Pb–Hf isotope systematics of the Jack Hills zircons. Earth Planet. Sci. Lett. 296, 45–56.
Kostrovitsky, S.I., Skuzovatov, S.Y., Yakovlev, D.A., Sun, J., Nasdala, L., Wu, F.Y., 2016. Age of the Siberian craton crust beneath the northern kimberlite ffelds: Insights to the craton evolution. Gondwana Res. 39, 365–385.
Lai, S.C., Li, Y.F., Qin, J.F., 2007. Geochemistry and LA-ICP-MS zircon U-Pb dating of the Dongjiahe ophiolite complex from the western Bikou terrane. Sci. China Earth Sci. 50, 305–313.
Li, Z.X., Kinny, P.D., 2002. Grenvillian continental collision in South China: new SHRIMP U-Pb zircon results and implications for the configuration of Rodinia. Geology 30, 163–166.
Li, L.M., Lin, S.F., Davis, D.W., Xiao, W.J., Xing, G.F., Yin, C.Q., 2014. Geochronology and geochemistry of igneous rocks from the Kongling terrane: Implications for Mesoarchean to Paleoproterozoic crustal evolution of the Yangtze Block. Precambr. Res. 255, 30–47.
Li, Z.C., Pei, X.Z., Li, R.B., Pei, L., Liu, C.J., Chen, G.C., Chen, Y.X., Xu, T., Yang, J., Wei, B., 2013b. Geochronological and geochemical study on Datan granite in Liujiaping area, northwest Yangtze Block and its tectonic setting. Geol. Rev. 59 (5), 869–884 in Chinese with an English abstract.
Li, L.S., Wang, X.L., Yakymchuk, C., Schorn, S., Yu, J.H., Wang, D., Li, J.Y., Du, D.H., Huang, Y., 2022. A refined study of Paleoproterozoic high-pressure granulite-facies metamorphism in the Kongling complex of northern Yangtze block. Precambr. Res. 378, 106741.
Li, H.K., Zhang, C.L., Yao, C.Y., Xiang, Z.Q., 2013a. U-Pb zircon age and Hf isotope compositions of Mesoproterozoic sedimentary strata on the western margin of the Yangtze massif. Sci. China Earth Sci. 56, 628–639.
Li, Y.H., Zheng, J.P., Ping, X.Q., Xiong, Q., Xiang, L., Zhang, H., 2018. Complex growth and reworking processes in the Yangtze cratonic nucleus. Precambr. Res. 311, 262–277.
Ling, W.L., Gao, S., Cheng, J.P., Jiang, L.S., Yuan, H.L., Hu, Z.C., 2006. Neoproterozoic magmatic events within the Yangtze continental interior and along its northern margin and their tectonic implication: Constraint from the ELA-ICPMS U-Pb geochronology of zircons from the Huangling and Hannan complexes. Acta Geol. Sin. 22, 387–396 in Chinese with an English abstract.
Liu, Y., Liu, X.M., Hu, Z.C., Diwu, C.R., Yuan, H.L., Gao, S., 2007. Evaluation of accuracy and long-term stability of determination of 37 trace elements in geological samples by ICP-MS. Acta Petrol. Sin. 23 (5), 1203–1210.
Liu, G.C., Qian, X., Li, J., Zi, J.W., Zhao, T.Y., Feng, Q.L., Chen, G.Y., Hu, S.B., 2020. Geochronological and geochemical constraints on the petrogenesis of early Paleoproterozoic (2.40-2.32 Ga) Nb-enriched mafic rocks in southwestern Yangtze Block and its tectonic implications. J. Earth Sci. 31 (1), 35–52.
Liu, G.C., Li, J., Qian, X., Feng, Q.L., Wang, W., Chen, G.Y., Hu, S.B., 2021. Geochronological and geochemical constraints on the petrogenesis of late Mesoproterozoic mafic and granitic rocks in the southwestern Yangtze Block. Geosci. Front. 12 (1), 39–52.
Liu, B., Zhai, M.G., Zhao, L., Cui, X.H., 2019. Metamorphism, P-T path and zircon U-Pb dating of Paleoproterozoic mafic and felsic granulites from the Kongling terrane. South China. Precambrian Res. 333, 105403.
Lu, G.M., Wang, W., Ernst, R.E., Söderlund, U., Lan, Z.F., Huang, S.F., Xue, E.K., 2019. Petrogenesis of Paleo-Mesoproterozoic mafic rocks in the southwestern Yangtze Block of South China: Implications for tectonic evolution and paleogeographic reconstruction. Precambr. Res. 322, 66–84.
Lu, G.M., Wang, W., Cawood, P.A., Ernst, R.E., Raveggi, M., Huang, S.F., Xue, E.K., 2020. Late Paleoproterozoic to Early Mesoproterozoic mafic magmatism in the SW Yangtze Block: Mantle plumes associated with Nuna breakup? J. Geophys. Res. Solid Earth 125 e2019JB019260.
Ludwig, K.R., 2003. User's manual for ISOPLOT/EX, version 3. A geochronological toolkit for Microsoft Excel. Berkeley Geochronol. Cent. Spec. Publ, Berkeley, p. 71.
Lupulescu, M.V., Chiarenzelli, J.R., Fisher, C.M., Hanchar, J.M., Bailey, D.G., 2023. Xenocrystic zircon in Central New York State kimberlites record Neoproterozoic disturbance of Grenville basement rocks. Lithos 456, 107303.
Meert, J.G., Santosh, M., 2017. The Columbia supercontinent revisited. Gondwana Res. 50, 67–83.
Miller, J.S., Matzel, J.E., Miller, C.F., Burgess, S.D., Miller, R.B., 2007. Zircon growth and recycling during the assembly of large, composite arc plutons. J. Volcanol. Geotherm. Res. 167 (1), 282–299.
Moyen, J.F., Paquette, J.L., Ionov, D.A., Gannoun, A., Korsakov, A.V., Golovin, A.V., Moine, B.N., 2017. Paleoproterozoic rejuvenation and replacement of Archaean lithosphere: Evidence from zircon U-Pb dating and Hf isotopes in crustal xenoliths at Udachnaya. Siberian Craton. Earth Planet. Sci. Lett. 457, 149–159.
Nie, H., Yao, J., Wan, X., Zhu, X.Y., Siebel, W., Chen, F.K., 2016. Precambrian tectonothermal evolution of South Qinling and its affnity to the Yangtze Block: Evidence from zircon ages and Hf–Nd isotopic compositions of basement rocks. Precambr. Res. 286, 167–179.
O'Reilly, S.Y., Griffin, W.L., Pearson, N.J., Jackson, S.E., Belousova, E.A., Alard, O., Saeed, A., 2008. Taking the pulse of the Earth: linking crustal and mantle events. Aust. J. Earth Sci. 55 (6–7), 983–995.
Page, F.Z., Fu, B., Kita, N.T., Fournelle, J., Spicuzza, M.J., Schulze, D.J., Viljoen, F., Basei, M.A., Valley, J.W., 2007. Zircons from kimberlite: new insights from oxygen isotopes, trace elements, and Ti in zircon thermometry. Geochim. Cosmochim. Acta 71 (15), 3887–3903.
Pearce, J.A., 2008. Geochemical fingerprinting of oceanic basalts with applications to ophiolite classification and the search for Archean oceanic crust. Lithos 100, 14–48.
Peng, M., Wu, Y.B., Gao, S., Zhang, H.F., Wang, J., Liu, X.C., Gong, H.J., Zhou, L., Hu, Z. C., Liu, Y.S., Yuan, H.L., 2012. Geochemistry, zircon U-Pb age and Hf isotope compositions of Paleoproterozoic aluminous A-type granites from the Kongling terrain, Yangtze Block: Constraints on petrogenesis and geologic implications. Gondwana Res. 22, 140–151.
Ping, X.Q., Zheng, J.P., Xiong, Q., Zhang, Z.H., Xia, B., 2014. Zircon U-Pb ages and Hf isotope characteristics of the granitic plutons in Bikou Terrane, northwestern Yangtze Block, and their geological significance. J. Jilin Univ. Earth Sci. Ed. 44, 1200–1218 in Chinese with an English abstract.
Polat, A., Hofmann, A.W., 2003. Alteration and geochemical patterns in the 3.7–3.8 Ga Isua greenstone belt, West Greenland. Precambr. Res. 126 (3–4), 197–218.
Qiu, X.F., Ling, W.L., Liu, X.M., Kusky, T., Berkana, W., Zhang, Y.H., Gao, Y.J., Lu, S.S., Kuang, H., Liu, C.X., 2011. Recognition of Grenvillian volcanic suite in the Shennongjia region and its tectonic significance for the South China Craton. Precambr. Res. 191, 101–119.
Qiu, X.F., Ling, W.L., Liu, X.M., Lu, S.S., Jiang, T., Wei, Y.X., Peng, L.H., Tan, J.J., 2018. Evolution of the Archean continental crust in the nucleus of the Yangtze block: Evidence from geochemistry of 3.0 Ga TTG gneisses in the Kongling high-grade metamorphic terrane. South China. J. Asian Earth Sci. 154, 149–161.
Ringwood, A.E., 1990. Slab–mantle interactions: 3. Petrogenesis of intraplate magmas and structure of the upper mantle. Chem. Geol. 82, 187–207.
Rudnick, R.L., Gao, S., 2014. Composition of the continental crust. In: Holland, H., Turekian, K. (Eds.), Treatise on Geochemistry. Elsevier, Holland, pp. 163–187.
Shakerardakani, F., Li, X.H., Ling, X.X., Li, J., Tang, G.Q., Liu, Y., Monfaredi, B., 2019. Evidence for Archean crust in Iran provided by ca. 2.7 Ga zircon xenocrysts within amphibolites from the Sanandaj-Sirjan zone, Zagros orogen. Precambrian Res. 332, 105390.
Shen, L.J., Chen, F.L., Wang, J., Cui, X.Z., Ren, G.M., Sun, Z.M., Pang, W.H., Ren, F., 2023. Paleo-Mesoproterozoic meta-basalts within the Caiziyuan-Tongan accretionary complex in the southwestern Yangtze Block, South China: Evidence for the breakup of the Nuna supercontinent. J. Asian Earth Sci. 251, 105660.
Shu, L.S., Wang, J.Q., Yao, J.L., 2019. Tectonic evolution of the eastern Jiangnan region, South China: New findings and implications on the assembly of the Rodinia supercontinent. Precambr. Res. 322, 42–65.
Siebel, W., Schmitt, A.K., Danišík, M., Chen, F.K., Meier, S., Weiß, S., Eroğlu, S., 2009. Prolonged mantle residence of zircon xenocrysts from the western Eger rift. Nat. Geosci. 2, 886–890.
Stern, R.J., Ali, K.A., Liégeois, J.P., Johnson, P.R., Kozdroj, W., Kattan, F.H., 2010. Distribution and significance of pre-Neoproterozoic zircons in juvenile Neoproterozoic igneous rocks of the Arabian-Nubian Shield. Am. J. Sci. 310 (9), 791–811.
Sun, M., Chen, N.S., Zhao, G.C., Wilde, S.A., Ye, K., Guo, J.H., Chen, Y., Yuan, C., 2008. U-Pb zircon and Sm-Nd isotopic study of the Huangtuling granulite, Dabie-Sulu belt,

China: implication for the Paleoproterozoic tectonic history of the Yangtze Craton. Am. J. Sci. 308, 469–483.
Sun, X.H., Luan, Y., Zhang, T.Y., Brzozowski, M.J., Ye, H., Wu, C.Z., 2022. Geochemistry, zircon U-Pb chronology and Hf isotope composition of the Heishan'gou iron deposit in the Bikou Terrane, central China: Implication for the genesis of the Yudongzi banded iron formations. Ore Geol. Rev. 152, 105250.
Sun, S.S., McDonough, W.F., 1989. Chemical and isotopic systematics of oceanic basalts: implications for mantle composition and processes. Geol. Soc. London Spec. Publ. 42, 313–345.
Taylor, S.R., McLennan, S.M., 1985. In: The Continental Crust: Its Evolution and Composition. Blackwell, London, p. 312.
Wang, Z.J., Deng, Q., Duan, T.Z., Yang, F., Du, Q.D., Xiong, X.H., Liu, H., Cao, B.F., 2018b. 2.85 Ga and 2.73 Ga A-type granites and 2.75 Ga trondhjemite from the Zhongxiang Terrain: Implications for early crustal evolution of the Yangtze Craton. South China. Gondwana Res. 61, 1–19.
Wang, K., Dong, S.W., 2019. New insights into Paleoproterozoic tectonics of the Yangtze Block in the context of early Nuna assembly: Possible collisional granitic magmatism in the Zhongxiang Complex. South China. Precambr. Res. 334, 105452.
Wang, K., Dong, S.W., Li, Z.X., Han, B.F., 2018a. Age and chemical composition of Archean metapelites in the Zhongxiang Complex and implications for early crustal evolution of the Yangtze Craton. Lithos 320, 280–301.
Wang, X.C., Li, X.H., Li, W.X., Li, Z.X., Liu, Y., Yang, Y.H., Liang, X.R., Tu, X.L., 2008. The Bikou basalts in the northwestern Yangtze block, South China: Remnants of 820–810 Ma continental flood basalts? Bull. Geol. Soc. Am. 120, 1478–1492.
Wang, K., Li, Z.X., Dong, S.W., Cui, J.J., Han, B.F., Zheng, T., Xu, Y.L., 2018c. Early crustal evolution of the Yangtze Craton, South China: New constraints from zircon U-Pb-Hf isotopes and geochemistry of ca. 2.9–2.6 Ga granitic rocks in the Zhongxiang Complex. Precambrian Res. 314, 325–352.
Wang, K., Dong, S.W., Yao, W.H., Zhang, Y.Q., Li, J.H., Cui, J.J., Han, B.F., 2020. Xenocrystic/inherited Precambrian zircons entrained within igneous rocks from eastern South China: Tracking unexposed ancient crust and implications for late Paleoproterozoic orogenesis. Gondwana Res. 84, 194–210.
Wang, Z.Z., Guo, Y., Yang, B., Wang, S.W., Sun, X.M., Hou, L., Zhou, B.G., Liao, Z.W., 2013c. Discovery of the 1.73 Ga Haizi anorogenic type granite in the western margin of Yantze Craton, and its geological significance. Acta Geol. Sin. 87 (7), 931–942 in Chinese with an English abstract.
Wang, W., Liu, S.W., Feng, Y.F., Li, Q.F., Wu, F.H., Wang, Z.Q., Wang, R.T., Yang, P.T., 2012. Chronology, petrogenesis and tectonic setting of the Neoproterozoic Tongchang dioritic pluton at the northwestern margin of the Yangtze Block: constraints from geochemistry and zircon U-Pb-Hf isotopic systematics. Gondwana Res. 22, 699–716.
Wang, Z.J., Wang, J., Du, Q.D., Deng, Q., Yang, F., 2013b. The evolution of the Central Yangtze Block during early Neoarchean time: evidence from geochronology and geochemistry. J. Asian Earth Sci. 77, 31–44.
Wang, Z.J., Wang, J., Deng, Q., Du, Q.D., Zhou, X.L., Yang, F., Liu, H., 2015. Paleoproterozoic I-type granites and their implications for the Yangtze block position in the Columbia supercontinent: evidence from the Lengshui Complex, South China. Precambr. Res. 263, 157–173.
Wang, Y.J., Zhang, A.M., Cawood, P.A., Fan, W.M., Xu, J.F., Zhang, G.W., Zhang, Y.Z., 2013a. Geochronological, geochemical and Nd-Hf-Os isotopic fingerprinting of an early Neoproterozoic arc-back-arc system in South China and its accretionary assembly along the margin of Rodinia. Precambr. Res. 231, 343–371.
Wang, W., Zhou, M.F., Zhao, X.F., Chen, W.T., Yan, D.P., 2014. Late Paleoproterozoic to Mesoproterozoic rift successions in SW China: Implication for the Yangtze Block-North Australia-Northwest Laurentia connection in the Columbia supercontinent. Sediment. Geol. 309, 33–47.
Wang, W., Cawood, P.A., Zhou, M.F., Zhao, J.H., 2016. Paleoproterozoic magmatic and metamorphic events link Yangtze to northwest Laurentia in the Nuna supercontinent. Earth Planet. Sci. Lett. 433, 269–279.
Wang, Y.J., Zhu, W.G., Huang, H.Q., Zhong, H., Bai, Z.J., Fan, H.P., Yang, Y.J., 2019. Ca. 1.04 Ga hot Grenville granites in the western Yangtze Block, southwest China. Precambr. Res. 328, 217–234.
Wei, J.Q., Jing, M.M., 2013. Chronology and geochemistry of amphibolites from the Kongling complex. Chin. J. Geol. 48, 970–983 in Chinese with English abstract.
Wilson, M., 1989. Igneous petrogenesis. Springer Netherlands, Dordrecht, 133 and 227–241 pp.
Winchester, J.A., Floyd, P.A., 1977. Geochemical discrimination of different magma series and their differentiation products using immobile elements. Chem. Geol. 20, 325–343.
Woodhead, J., Hergt, J., Giuliani, A., Phillips, D., Maas, R., 2017. Tracking continental scale modification of the Earth's mantle using zircon megacrysts. Geochem. Perspect. Lett. 4, 1–6.
Wu, Y.B., Gao, S., Gong, H.J., Xiang, H., Jiao, W.F., Yang, S.H., Liu, Y.S., Yuan, H.L., 2009. Zircon U-Pb age, trace element and Hf isotope composition of Kongling terrane in the Yangtze Craton: Refining the timing of Palaeoproterozoic high-grade metamorphism. J. Metamorph. Geol. 27, 461–477.
Wu, Y.B., Gao, S., Zhang, H.F., Zheng, J.P., Liu, X.C., Wang, H., Gong, H.J., Zhou, L., Yuan, H.L., 2012. Geochemistry and zircon U-Pb geochronology of Paleoproterozoic arc related granitoid in the Northwestern Yangtze Block and its geological implications. Precambr. Res. 200–203, 26–37.
Wu, F.Y., Yang, Y.H., Xie, L.W., Yang, J.H., Xu, P., 2006. Hf isotopic compositions of the standard zircons and baddeleyites used in U-Pb geochronology. Chem. Geol. 234, 105–126.
Wu, Y.B., Zheng, Y.F., 2004. Genesis of zircon and its constraints on interpretation of U-Pb age. Chin. Sci. Bull. 49 (15), 1554–1569.
Wu, Y.B., Zheng, Y.F., Gao, S., Jiao, W.F., Liu, Y.S., 2008. Zircon U-Pb age and trace element evidence for Paleoproterozoic granulite-facies metamorphism and Archean crustal rocks in the Dabie Orogen. Lithos 101, 308–322.
Wu, Y.B., Zhou, G.Y., Gao, S., Liu, X.C., Qin, Z.W., Wang, H., Yang, J.Z., Yang, S.H., 2014. Petrogenesis of Neoarchean TTG rocks in the Yangtze Craton and its implication for the formation of Archean TTGs. Precambrian Res. 254, 73–86.
Xia, L.Q., Xia, Z.C., Xu, X.Y., 1996. Properties of middle-late Proterozoic volcanic rocks in South Qinling and the Precambrian continental break-up. Sci. China Earth Sci. 39 (3), 256–265 in Chinese with an English abstract.
Xia, L.Q., Xia, Z.C., Xu, X.Y., Li, X.M., Ma, Z.P., 2007. Petrogenesis of the Bikou Group volcanic rocks. Earth Sci. Front. 14 (3), 84–101 in Chinese with an English abstract.
Xiao, L., Zhang, H.F., Ni, P.Z., Xiang, H., Liu, X.M., 2007. LA-ICP-MS U-Pb zircon geochronology of early Neoproterozoic mafic-intermediat intrusions from NW margin of the Yangtze Block, South China: Implication for tectonic evolution. Precambr. Res. 154, 221–235.
Xiong, Q., Zheng, J.P., Yu, C.M., Su, Y.P., Tang, H.Y., Zhang, Z.H., 2008. Zircon U-Pb age and Hf isotope of Quanyishang A-type granite in Yichang: Significance for the Yangtze continental cratonization in Paleoproterozoic. Chin. Sci. Bull. 54, 436–446.
Xu, X.Y., Xia, Z.C., Xia, L.Q., 2002. Volcanic cycles of the Bikou Group and their tectonic implications. Geol. Bull. China 21, 478–485 in Chinese with an English abstract.
Yan, Q.R., Wang, Z.Q., Yan, Z., Hanson, A.D., Druschke, P.A., Liu, D.Y., Song, B., Jian, P., Wang, T., 2003. The age of the Bikou Group volcanic rock: Evidence from Zircon SHRIMP U-Pb dating results. Geol. Bull. China 22 (6), 456–458 in Chinese with an English abstract.
Yan, Q.R., Andrew, D.H., Wang, Z.Q., Yan, Z., Peter, A.D., Wang, T., Liu, D.Y., Song, B., Jiang, C.F., 2004a. Geochemistry and tectonic setting of the Bikou volcanic terrane on the northern margin of the Yangtze plate. Acta Petrol. Mineral. 23, 1–11 in Chinese with an English abstract.
Yan, Q.R., Hanson, A.D., Wang, Z.Q., Druschke, P.A., Yan, Z., Wang, T., Liu, D.Y., Song, B., Jian, P., Zhou, H., Jiang, C.F., 2004b. Neoproterozoic Subduction and Rifting on the Northern Margin of the yangtze Plate, China: Implications for Rodinia Reconstruction. Int. Geol. Rev. 46, 817–832.
Yang, B., Dong, G.C., Guo, Y., Wang, Z.Z., Wang, P., 2016. Geochemistry, zircon U-Pb geochronology and significances of the Dazhupeng rhyolites in the western Yangtze Platform. J. Mineral. Petrol. 36 (2), 82–91 in Chinese with an English abstract.
Yang, H., Liu, F.L., Du, L.L., Liu, P.H., Wang, F., 2012. Zircon U-Pb dating for metavolcanites in the laochanghe Formation of the Dahongshan Group in southwestern Yangtze Block, and its geological significance. Acta Petrol. Sin. 28 (9), 2994–3014 in Chinese with an English abstract.
Yang, Z., Zi, J.W., Cawood, P.A., Zhao, T.Y., Liu, G.C., Li, J., Zhang, H., Wei, Y.H., Feng, Q.L., 2023. A refined Archean-Paleoproterozoic magmatic framework of the Cuoke Complex, SW China, and its implications for early Precambrian evolution of the Yangtze Block. Precambr. Res. 384, 106921.
Yao, J.L., Cawood, P.A., Shu, L.S., Zhao, G.C., 2019. Jiangnan Orogen, South China: A ~970–820 Ma Rodinia margin accretionary belt. Earth-Sci. Rev. 196, 102872.
Yin, C.Q., Lin, S.F., Davis, D.W., Zhao, G.C., Xiao, W.J., Li, L.M., He, Y.H., 2013. 2.1-1.85 Ga tectonic events in the Yangtze Block South China: petrological and geochronological evidence from the Kongling Complex and implications for the reconstruction of supercontinent Columbia. Lithos 182–183, 200–210.
Zhai, M.G., Guo, J.H., Liu, W.J., 2005. Neoarchean to Paleoproterozoic continental evolution and tectonic history of the North China Craton: A review. J. Asian Earth Sci. 24, 547–561.
Zhang, C.H., Gao, L.Z., Wu, Z.J., Shi, X.Y., Yan, Q.R., Li, D.J., 2007. SHRIMP U-Pb zircon age of tuff from the Kunyang Group in central Yunnan: evidence for Grenvillian orogeny in South China. Chin. Sci. Bull. 52, 1517–1525.
Zhang, L.J., Ma, C.Q., Wang, L.X., She, Z.B., Wang, S.M., 2011. Discovery of Paleoproterozoic rapakivi granite on the northern margin of the Yangtze block and its geological significance. Chin. Sci. Bull. 1 (3), 306–318.
Zhang, A.M., Wang, Y.J., Fan, W.M., Zhang, Y.Z., Yang, J., 2012. Earliest Neoproterozoic (ca. 1.0 Ga) arc–back-arc basin nature along the northern Yunkai Domain of the Cathaysia Block: Geochronological and geochemical evidence from the metabasite. Precambr. Res. 220–221, 217–233.
Zhang, J.J., Wang, T., Zhang, L., Tong, Y., Zhang, Z.C., Shi, X.C., Shi, X.J., Guo, L., Huang, H., Yang, Q.D., Huang, W., Zhao, J.X., Ye, K., Zhao, J.Y., 2015. Tracking deep crust by zircon xenocrysts within igneous rocks from the northern Alxa, China: Constraints on the southern boundary of the Central Asian Orogenic Belt. J. Asian Earth Sci. 108, 150–169.
Zhang, X., Xu, X.Y., Song, G.S., Wang, H.L., Chen, J.L., Li, T., 2010. Zircon LA-ICP-MS U-Pb dating and significance of Yudongzi Group deformation granite from Lueyang area, western Qinling. China. Geol. Bull. China 29, 510–517. In Chinese with English abstract.
Zhang, Z.Q., Zhang, G.W., Tang, S.H., Wang, J.H., 2001. On the age of metamorphic rocks of the Yudongzi Group and the Archean crystalline basement of the Qinling Orogen. Acta Geol. Sin. 75, 198–204 in Chinese with an English abstract.
Zhang, S.B., Zheng, Y.F., Wu, Y.B., Zhao, Z.F., Gao, S., Wu, F.Y., 2006b. Zircon isotope evidence for ≥3.5 Ga continental crust in the Yangtze craton of China. Precambr. Res. 146, 16–34.
Zhang, S.B., Zheng, Y.F., Wu, Y.B., Zhao, Z.F., Gao, S., Wu, F.Y., 2006c. Zircon U-Pb age and Hf-O isotope evidence for Paleoproterozoic metamorphic event in South China. Precambr. Res. 151, 265–288.
Zhang, S.B., Zheng, Y.F., 2013. Formation and evolution of Precambrian continental lithosphere in South China. Gondwana Res. 23, 1241–1260.
Zhang, S.B., Zheng, Y.F., Wu, Y.B., Zhao, Z.F., Gao, S., Wu, F.Y., 2006a. Zircon U-Pb age and Hf isotope evidence for 3.8 Ga crustal remnant and episodic reworking of Archean crust in South China. Earth Planet. Sci. Lett. 252, 56–71.

Zhang, S.B., Zheng, Y.F., Wu, P., He, Q., Rong, W., Fu, B., Yang, Y.H., Liang, T., 2020. The nature of subduction system in the Neoarchean: Magmatic records from the northern Yangtze Craton. South China. Precambrian Res. 347, 105834.
Zhao, M., 2013. Huangling mafic crystalline basement-zircon age and significance of ultramafic rocks. A Dissertation Submitted to Northwest University for Master's Degree (in Chinese with English Abstract).
Zhao, J.H., Asimow, P.D., 2018. Formation and evolution of a magmatic system in a rifting continental margin: Neoproterozoic Arc- and MORB-like dike swarms in South China. J. Petrol. 59, 1811–1844.
Zhao, G.C., Cawood, P.A., Wilde, S.A., Sun, M., 2002. Review of global 2.1-1.8 Ga orogens: implications for a pre-Rodinia supercontinent. Earth Sci. Rev. 59, 125–162.
Zhao, G.C., Cawood, P.A., 2012. Precambrian Geology of China. Precambr. Res. 222–223, 13–54.
Zhao, L., Guo, F., Fan, W.M., Huang, M.W., 2019. Roles of subducted pelagic and terrigenous sediments in Early Jurassic mafic magmatism in NE China: Constraints on the architecture of Paleo-Pacific subduction zone. J. Geophys. Res.: Solid. Earth 124, 2525–2550.
Zhao, T.Y., Li, J., Liu, G.C., Cawood, P.A., Zi, J.W., Wang, K., Feng, Q.L., Hu, S.B., Zeng, W.T., Zhang, H., 2020. Petrogenesis of Archean TTGs and potassic granites in the southern Yangtze Block: Constraints on the early formation of the Yangtze Block. Precambr. Res. 347, 105848.
Zhao, X.S., Ma, S.L., Zou, X.S., Xiu, Z.L., 1990. The study of the age, sequence, volcanism and mineralization of Bikou Group in Qinling-Dabashan. Bull. Xi'an Inst. Geol. Min. Res., Chinese Acad. Geol. Sci, No. 29, 1–121 in Chinese.
Zhao, G.C., Sun, M., Wilde, S.A., Li, S.Z., 2004. A Paleo-Mesoproterozoic supercontinent: Assembly, growth and breakup. Earth Sci. Rev. 67 (1–2), 91–123.
Zhao, J.H., Zhou, M.F., 2008. Neoproterozoic adakitic plutons in the northern margin of the Yangtze Block, China: Partial melting of a thickened lower crust and implications for secular crustal evolution. Lithos 104, 231–248.
Zhao, X.F., Zhou, M.F., 2011. Fe–Cu deposits in the Kangdian region, SW China: a Proterozoic IOCG (iron-oxide-copper-gold) metallogenic province. Miner. Deposita 46, 731–747.
Zhao, X.F., Zhou, M.F., Li, J.W., Sun, M., Gao, J.F., Sun, W.H., Yang, J.H., 2010. Late Paleoproterozoic to early Mesoproterozoic Dongchuan Group in Yunnan, SW China: Implications for tectonic evolution of the Yangtze Block. Precambrian Res. 182 (1), 57–69.
Zheng, J.P., Griffin, W.L., O'Reilly, S.Y., Zhang, M., Pearson, N., Pan, Y.M., 2006. Widespread Archean basement beneath the Yangtze Craton. Geology 34, 417–420.
Zheng, J.P., Griffin, W.L., O'Reilly, S.Y., Zhao, J.H., Wu, Y.B., Liu, G.L., Pearson, N.J., Zhang, M., Ma, C.Q., Zhang, Z.H., Yu, C.M., Su, Y.P., Tang, H.Y., 2009. Neoarchean (2.7–2.8 Ga) accretion beneath the North China Craton: U-Pb age, trace elements and Hf isotopes of zircons in diamondiferous kimberlites. Lithos 112, 188–202.
Zheng, J.P., Griffin, W.L., Ma, Q., O'Reilly, S.Y., Xiong, Q., Tang, H.Y., Zhao, J.H., Yu, C. M., Su, Y.P., 2012. Accretion and reworking beneath the North China Craton. Lithos 149, 61–78.
Zheng, Y.F., Xiao, W.J., Zhao, G.C., 2013. Introduction to tectonics of China. Gondwana Res. 23, 1189–1206.
Zhou, M.F., Kennedy, A.K., Sun, M., Malpas, J., Lesher, C.M., 2002. Neoproterozoic arc-related mafic intrusions along the northern margin of South China: Implications for the accretion of Rodinia. J. Geol. 110, 611–618.
Zhou, G.Y., Wu, Y.B., Gao, S., Yang, J.Z., Zheng, J.P., Qin, Z.W., Wang, H., Yang, S.H., 2015. The 2.65 Ga A-type granite in the northeastern Yangtze craton: petrogenesis and geological implications. Precambr. Res. 258, 247–259.
Zhou, G.Y., Wu, Y.B., Wang, H., Qin, Z.W., Zhang, W.X., Zheng, J.P., Yang, S.H., 2017. Petrogenesis of the Huashanguan A-type granite complex and its implications for the early evolution of the Yangtze Block. Precambr. Res. 292, 57–74.
Zhou, G.Y., Wu, Y.B., Li, L., Zhang, W.X., Zheng, J.P., Wang, H., Yang, S.H., 2018. Identiffcation of ca. 2.65 Ga TTGs in the Yudongzi complex and its implications for the early evolution of the Yangtze Block. Precambr. Res. 314, 240–263.
Zhou, M.F., Yan, D.P., Wang, C.L., Qi, L., Kennedy, A., 2006. Subduction-related origin of the 750 Ma Xuelongbao adakitic complex (Sichuan Province, China): implications for the tectonic setting of the giant Neoproterozoic magmatic event in South China. Earth Planet. Sci. Lett. 248, 286–300.
Zhou, M.F., Zhao, X.F., Chen, W.T., Li, X.C., Wang, W., Yan, D.P., Qiu, H.N., 2014. Proterozoic Fe-Cu metallogeny and supercontinental cycles of the southwestern Yangtze Block, southern China and northern Vietnam. Earth Sci. Rev. 1396, 59–82.
Zhu, W.G., Zhong, H., Li, Z.X., Bai, Z.J., Yang, Y.J., 2016. SIMS zircon U-Pb ages, geochemistry and Nd-Hf isotopes of ca. 1.0 Ga mafic dykes and volcanic rocks in the Huili area, SW China: origin and tectonic significance. Precambrian Res. 273, 67–89.
Zhu, W.G., Bai, Z.J., Zhong, H., Ye, X.T., Fan, H.P., 2017. The origin of the ca. 1.7 Ga gabbroic intrusion in the Hekou area, SW China: constraints from SIMS U-Pb zircon geochronology and elemental and Nd isotopic geochemistry. Geol. Mag. 154 (2), 286–304.